Research Highlights

[FY2024]

Japan International Research Center for Agricultural Sciences

Meeting global challenges through research and technology development

国際農研

Carbon sequestration and soil fertility management in sandy and clayey soils revealed by over four decades of long-term field experiments in Thailand

Since soil is the largest terrestrial carbon (C) reservoir, even small changes in soil C storage can significantly impact the global C cycle. To better understand soil C dynamics in agricultural soils, it is essential to conduct long-term field experiments on the effects of various land management practices on the same farmland. However, long-term field experiments in tropical regions are limited, making it difficult to assess the impact of agricultural management on soil C sequestration accurately. JIRCAS, in collaboration with the Department of Agriculture (DOA) of Thailand, has analyzed data from over 45 years of long-term field experiments involving the continuous application of chemical fertilizer and organic matter (OM) on cropland.

The data from three long-term field experiments (hereafter referred to as Khon Kaen, Nakhon Ratchasima, and Rayong) were analyzed. Compared to the control without any amendment, soil C sequestration was 2.0 ± 2.1 and 2.8 ± 2.0 Mg C ha^{-1} 0.2 m^{-1} for chemical fertilizer and crop residue incorporation, respectively. The largest soil C sequestration occurred when chemical fertilizers were combined with OM applications. Specifically, when chemical fertilizer was combined with crop residue incorporation or compost application, soil C sequestration reached 5.6 ± 3.1 and 10.1 ± 6.5 Mg C ha^{-1} 0.2 m^{-1}, respectively (Fig. 1). Furthermore, the trend of C sequestration varied depending on soil type. In clayey soils (Nakhon Ratchasima), C was concentrated in the surface layer, whereas in sandy soils (Khon Kaen), the effect was significant across all layers up to a depth of 1.0 m (Fig. 2). Structural equation modeling indicated that the increase in soil C in sandy soils significantly improved basal soil fertility, such as soil pH, available phosphorus, and exchangeable potassium, resulting in higher cassava yields (Fig. 3). In contrast, no significant relationship was found between soil C content and cassava yield in clayey soils.

These results are expected to contribute to the establishment of a soil C dynamics model optimized for tropical regions by providing reliable estimates of soil carbon sequestration rates in low-latitude regions, where studies have been limited. Furthermore, the Intergovernmental Panel on Climate Change (IPCC) sets the standard for soil carbon sequestration assessment at a depth of 0.3 m (or tillage depth) from the surface. The results of this study indicate that in sandy soils, it is necessary to evaluate even deeper layers.

Authors: Iwasaki S., Watanabe, T., Matsumoto N. [JIRCAS], Tancharoen, S., Luanmanee, S., Nobuntou, W., Amonpon, W., Chumsuwan, N., Paisancharoen, K., Bumrung, S. [DOA]

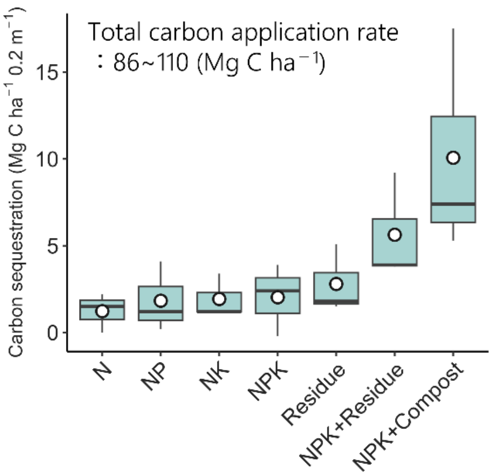

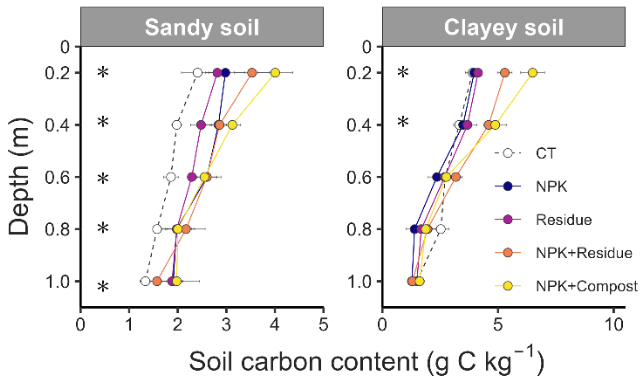

Fig. 1. Soil carbon sequestration rate

Calculated from long-term field experiments in Khon Kaen, Nakhon Ratchasima, and Rayong. Soil carbon sequestration is expressed as the difference from the control plot without any application. In the residue and NPK + residue treatments, cassava stems and leaves were returned to the field after harvest. The box plot represents the maximum, third quartile, median, first quartile, and minimum values. The ○ symbol indicates the mean value.

Fig. 2. Soil carbon content at five different depths

Soil samples were collected from five depth intervals (0–0.2 m, 0.2–0.4 m, 0.4–0.6 m, 0.6–0.8 m, and 0.8–1.0 m) in 2021. Values are presented as the mean ± standard error. The asterisk (*) indicates a significant difference between treatments at p < 0.05. Results from Khon Kaen represent sandy soil, while those from Nakhon Ratchasima represent clayey soil.

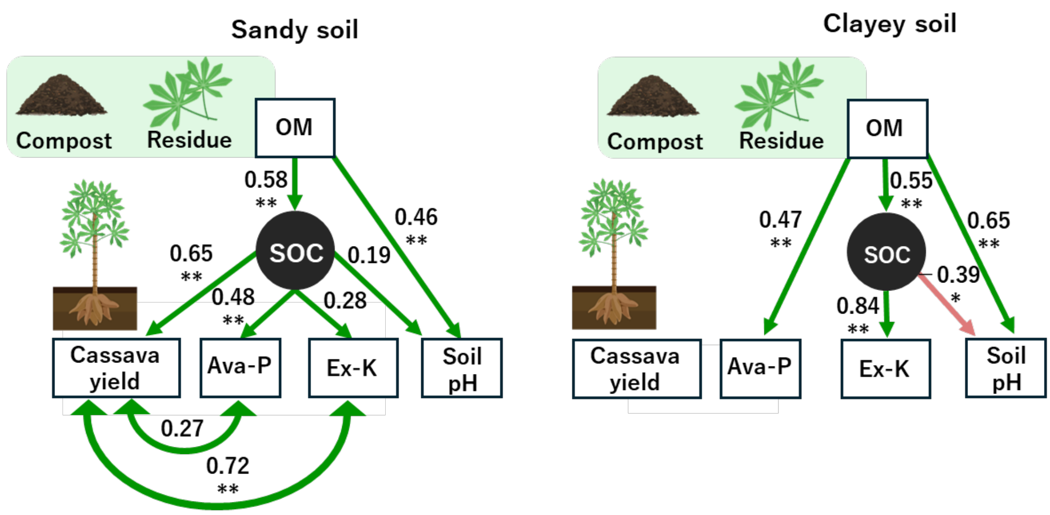

Fig. 3. Structural equation modeling of cassava yield

The relationships among organic matter application (OM), soil carbon concentration (SOC), available phosphorus (Ava-P), exchangeable potassium (Ex-K), soil pH, and cassava yield were analyzed using a structural equation model. Unidirectional arrows indicate causal relationships, while bidirectional arrows represent correlations. The numbers indicate the contribution coefficient. * and ** represent statistical significance at p < 0.05 and p < 0.01, respectively.

Reference: Tancharoen et al. (2024) *Land Degradation & Development* 35: 5488–5503.

The application of filter cakes improves the physicochemical and biological properties of soils with low pH in tropical regions

The application of organic matter is recommended for carbon sequestration and fertility improvement in agricultural soils. Sugarcane is widely cultivated in tropical regions, and a large amount of filter cake (FC) is produced as a by-product in the sugar industry. Earthworms (Oligochaeta) can improve soil functions such as nutrient cycling and water retention by promoting organic matter decomposition and modifying soil structure through their feeding and casting activities. Organic matter application is known to increase earthworm density and biomass. Also, soil pH can influence earthworm species composition, density, and biomass. However, the effects of organic amendments on these characteristics of earthworms at different soil pH values have not been fully understood, especially in tropical agricultural fields.

We conducted a field survey to evaluate the effects of a single application of FC on soil physicochemical properties and earthworm species, density, and biomass in sugarcane fields with two different soil pHs (low pH soil : <5.2, moderate pH soil : >6.0) on Ishigaki Island, Okinawa Prefecture, Japan. FC application decreased soil bulk density and hardness, and water content increased in the low pH soil. In addition, available P content and Ca^{2+}, K^{+}, and Mg^{2+} contents increased about 2-fold, and cation exchange capacity also increased (Table 1). In the moderate pH soil, FC application did not improve physical properties, although the available P increased 2.5-fold, and soil pH and Ca^{2+} and K^{+} contents decreased. Regardless of soil pH and FC application, *Pontoscolex corethrurus* (Müller, 1856) was dominant (Fig. 1) and accounted for approximately 30% to 100% of the density in each treatment. In addition to *P. corethrurus*, *Polypheretima elongata* (Perrier, 1872) was observed in the low pH soil with FC application. Earthworm biomass increased about 3-fold in the low pH soil but decreased by about 80% in the moderate pH soil with FC application (Fig. 2). Therefore, FC application to low pH soils can improve both physicochemical and biological properties of the soil.

Our results suggest that the application of FC, an underutilized organic resource, is expected to improve soil functions such as nutrient cycling and water retention in low pH soils through enhanced biological properties. Since this conclusion is based on data from a single application of FC, the effects of continuous application of FC and the effects of application of organic materials with different chemical properties from FC on soil physical and chemical properties need to be investigated. Additionally, future evaluations should include yield assessments.

Authors: Arai, M., Ikazaki, K., Terajima, Y., Anzai, T. [JIRCAS], Minamiya, Y. [Tochigi Pref. Museum]

Table 1. Effect of filter cake application on physicochemical properties of soils at low pH and moderate pH

Soil pH	FC	pH (H_2O)	EC	Bulk density	Water content	Hardness	TC	C:N ratio	Available P	Ca^{2+}	K^+	Mg^{2+}	CEC
			mS m^{-1}	Mg m^{-3}	m^3 m^{-3}	mm	g kg^{-1}		μg kg^{-1}	cmolc kg^{-1}	cmolc kg^{-1}	cmolc kg^{-1}	cmol(+) kg^{-1}
Low	No	4.74 (0.21)	6.35 (0.90)	1.22 (0.11)	0.21 (0.01)	12.32 (1.75)	9.69 (2.07)	9.89 (0.63)	115.6 (31.1)	1.74 (0.92)	0.27 (0.02)	0.42 (0.15)	13.22 (0.46)
	Yes	4.98 (0.38)	9.40 (2.33)	1.15 (0.14)	0.25 (0.02)	8.63 (0.98)	9.48 (1.55)	9.46 (0.41)	209.7 (21.1)	3.80 (1.39)	0.53 (0.19)	0.78 (0.14)	13.71 (2.65)
	p value		***	**	**	*		*	***	***	***	***	***
Moderate	No	6.50 (0.27)	6.76 (1.12)	1.20 (0.02)	0.22 (0.04)	7.40 (1.51)	9.19 (2.33)	9.82 (0.42)	125.7 (19.9)	10.25 (2.55)	0.61 (0.19)	1.33 (0.34)	16.60 (4.06)
	Yes	5.54 (0.20)	7.98 (1.27)	1.25 (0.16)	0.24 (0.03)	9.99 (3.13)	11.33 (2.17)	9.88 (0.29)	316.2 (67.6)	5.29 (1.27)	0.46 (0.06)	1.10 (0.13)	15.71 (2.93)
	p value	***							***	**	***		

Three pairs of adjacent sugarcane fields with and without filter cake application were selected in each of the low (< 5.2) and moderate (> 6.0) pH soils. FC: filter cake; EC: electrical conductivity; TC: total carbon content; C:N ratio: ratio of total carbon to total nitrogen. All cations are exchangeable. *$p < 0.05$; **$p < 0.01$; ***$p < 0.001$. Values represent the mean (standard error) of three experimental plots.

Fig. 1. Density of earthworms and proportion of each species in the density

The numbers at the top of the pie chart indicate the density (N m^{-2}), and the numbers within the pie chart indicate the proportion of each species in the density (%). Blue: *Pontoscolex corethrurus* (Müller, 1856), Green: *Polypheretima elongata* (Perrier, 1872), Red: *Dichogaster bolaui* (Michaelsen, 1891), White/Other: represents individuals for which species identification was not possible due to fragments. Earthworms were collected by hand sorting soil at 0–10 cm depth corresponding to Table 1 and by mustard solution at a depth deeper than 10 cm.

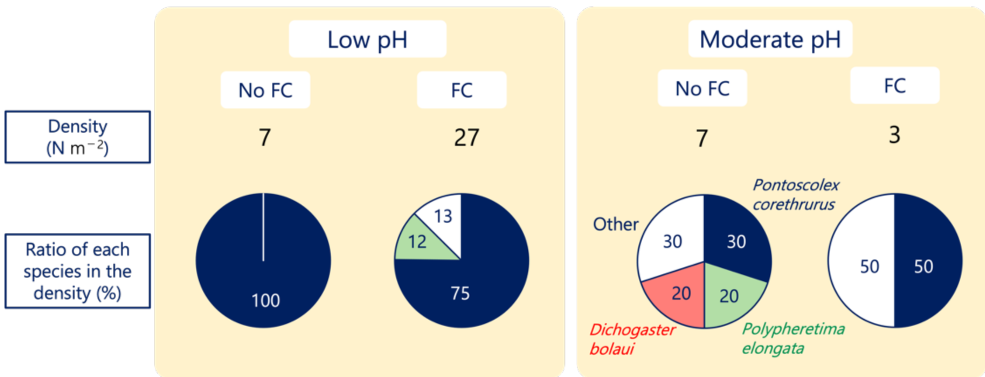

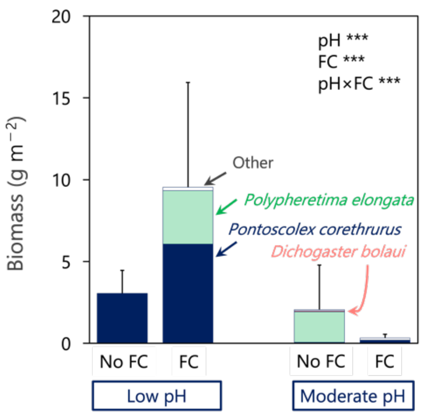

Fig. 2. Effect of filter cake application on earthworm biomass in each pH soil

Earthworm biomass for each species (g m^{-2}), corresponding to Figure 1 data. Error bars represent standard errors of total earthworm biomass in the three sugarcane fields. ***$p < 0.05$.

Reference: Arai et al. (2024) *European Journal of Soil Biology* 122: 103645.

Stabilization of soil organic matter by reactive aluminum phases in agricultural fields under volcanic influence

Increasing soil organic matter (SOM) storage in agricultural soils is needed to mitigate climate change and improve soil fertility. Particularly in humid tropical regions, high temperatures and high soil moisture can reduce SOM content. Understanding the factors that control SOM storage is a key step towards effective soil management for sustainable crop production. While clay + silt content is known to be an important factor in the stabilization of soil organic carbon (SOC)*, recent studies have shown that oxalate-extracted Al (reactive Al) is of greater importance. Reactive Al roughly corresponds to organo-Al complexes and amorphous clay**, and is formed through weathering of volcanic debris. However, in the tropics, most studies have been conducted on weathered soils with low reactive Al content, and the relationship between reactive Al and SOC content in different land uses has not been fully understood. This study aimed to clarify the factors regulating SOM content in agricultural fields compared to secondary forests or home gardens in Negros Occidental, Philippines. Sugarcane fields have been continuously cultivated for more than 70 years in the study site (Fig. 1).

SOC showed significant positive correlations with reactive Al content, but not with clay + silt content (Fig. 2). The slope of the regression line between SOC and reactive Al was not significantly different between sugarcane and the other two land uses, while the intercept was significantly lower in sugarcane sites (Fig. 3). These results suggest that land use conversion from forest to sugarcane decreases the SOC fraction (particulate organic matter***) that is relatively easily decomposed by soil microorganisms but does not decrease the SOC fraction stabilized by reactive Al.

Even in humid tropical regions where SOM is easily depleted, it is possible to achieve soil carbon sequestration in agricultural fields by developing technologies to increase the SOC fraction stabilized by reactive Al under volcanic influence. To develop such technologies, it would be necessary to evaluate the effects of factors (e.g., reactive Al content, SOC saturation level, quality and quantity of organic materials applied to fields) on the amount of change in SOC stabilized by reactive Al.

*Stabilization of SOM: resistance to decomposition by soil microorganisms

**Amorphous clay: general term for clay with low crystallinity

***Particulate organic matter: Coarse SOM derived from fallen leaves, dead roots, and dead soil animals

Authors: Arai, M., Ikazaki, K., Anzai T. [JIRCAS],
Celestial, P.V., Tumbay, V.J., Santillana, S.I. [SRA], Wagai, R. [NARO]

Fig. 1. Sampling points for each land use type

Sugarcane fields, secondary forests, and home gardens in Negros Occidental, Philippines

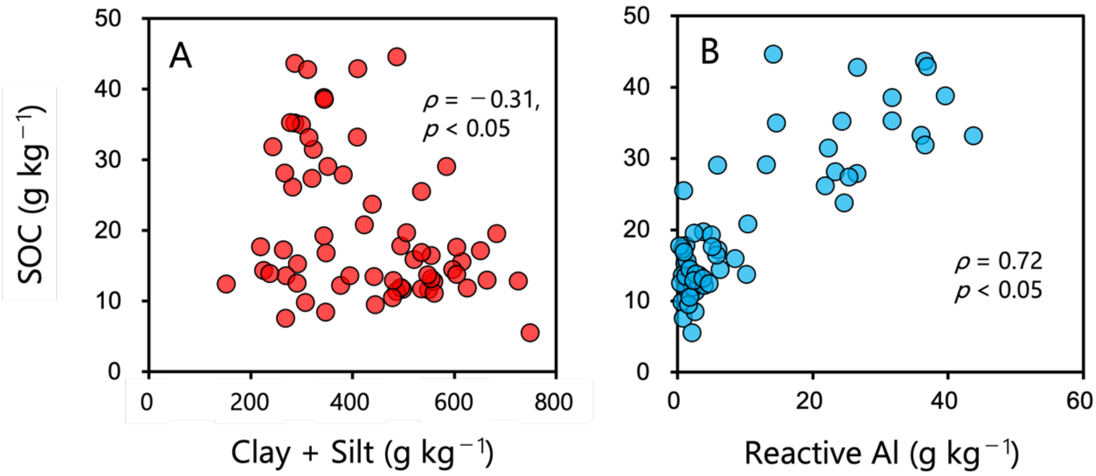

Fig. 2. Relationships between soil organic carbon (SOC) and clay + silt content (A) and reactive Al content (B)

Spearman's rank correlation coefficient (ρ) and *p* value are shown. Soils were collected at 0–10 cm depth from sugarcane fields (n = 33), secondary forests (n = 10), and home gardens (n = 23) in Negros Occidental, Philippines.

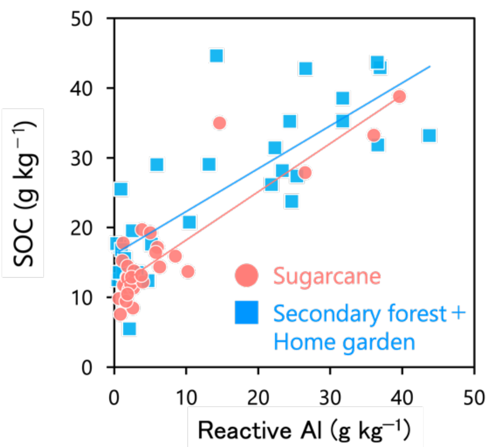

Fig. 3. Relationship between reactive Al content and SOC content by land use

Regression lines are shown for sugarcane fields (red; n = 33; y = 0.69x + 11.27, R^2 = 0.78, $p < 0.05$), which were highly anthropogenically disturbed, and other land uses (secondary forests + home gardens) (blue; n = 33; y = 0.61x + 16.16, R^2 = 0.78, $p < 0.05$), which were less disturbed. Analysis of covariance showed no significant difference in the slopes of the two regression lines ($p > 0.05$), but a significant difference in the intercepts ($p < 0.05$). This indicated that there was no difference in the SOC fraction stabilized by reactive Al between land uses.

Reference: Arai et al. (2025) *Soil Science and Plant Nutrition* 71: 27–37.

Enhancing reservoir water management through ratoon rice double cropping in tropical monsoon regions

Ratoon rice double cropping (RR) offers a resource-efficient alternative to conventional rice double cropping (DR) by eliminating the need for seedling preparation, puddling, and transplanting while also shortening the growth period. In irrigated areas under tropical monsoon climates, its adoption could contribute to stable water resource management. However, its impact on reservoir operations at the irrigation district level remains unverified. This study evaluates the effects of introducing RR on reservoir operations in the Yezin irrigation area of Myanmar, where dry-season water use is restricted due to hydrological variability, and wet-season cropping is prioritized.

This report estimates evapotranspiration for ratoon rice cropping using newly defined crop coefficients. Using 23 years of hydrological data, the reservoir water balance simulation was performed under different cropping patterns, including single, double, and triple cropping scenarios. Key indicators such as water shortage, reliability index (RAI), and water productivity (WP) were assessed. Additionally, rice yields were predicted using a machine learning model developed from 10 cropping trials, with input features such as harvest dates, meteorological data, and cutting heights. WP was calculated using simulated irrigation supply data (Fig. 1). For single rice cropping (3,600 ha in the wet season), early-season planting in early June avoids water shortages while maintaining WP of over 1.5 kg m^{-3} (Fig. 2). In DR, limiting the dry-season cultivation area to 1,400 ha (total annual cropping area, 5,000 ha) ensures an RAI above 0.8, a threshold for sustainable reservoir operations. In RR, planting in the dry season leads to water shortages that prevent crop continuation. However, when RR begins in the early wet season, an RAI above 0.8 is maintained. Compared to DR, WP improves by 60–87%, enabling more efficient reservoir management. However, for the triple rice-ratoon-ratoon cropping to maintain an RAI above 0.8, planting must be delayed with a cropping area of less than 4,400 ha, resulting in a reduction in WP to 0.45–0.48 kg m^{-3} (Fig. 3).

The proposed simulation framework enables comprehensive assessment of water shortage risks and WP in irrigated paddy rice under tropical climates. It facilitates the formulation of sustainable cropping and irrigation plans as an adaptation strategy to climate variability. For effective ratoon double cropping, strategies must be implemented to optimize harvesting schedules, avoiding rainfall-induced delays and mitigating yield losses from mechanical harvesting-related stubble compression.

Authors: Shiraki, S. [JIRCAS], Kywae, Nwe, N., Thin, M.C., Aung, K.T. [DAR]

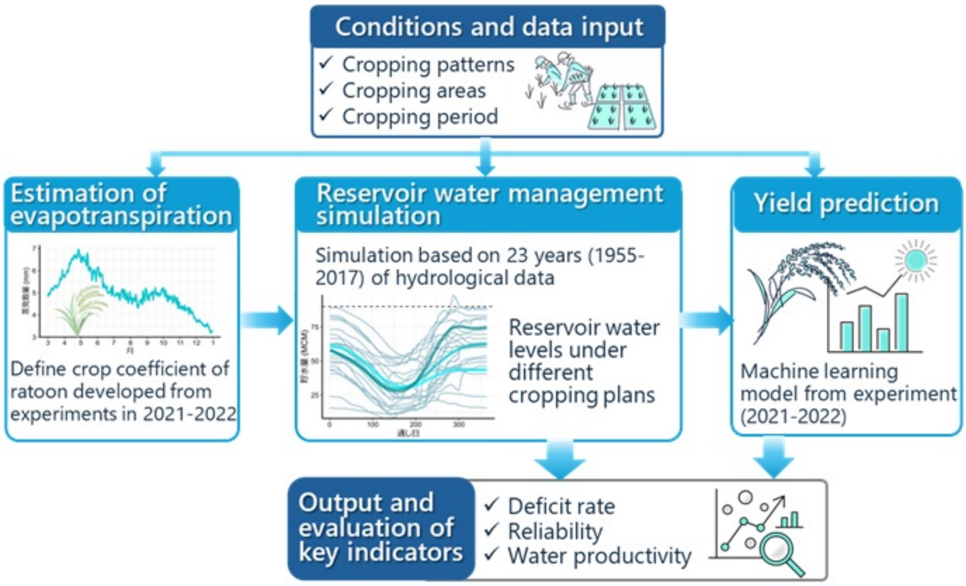

Fig. 1. Assessment of reservoir operations under different rice cropping patterns

In the study area, wet-season rice cropping (maximum area: 3600 ha) is prioritized, and dry-season cropping is adjusted based on early dry-season reservoir water levels.

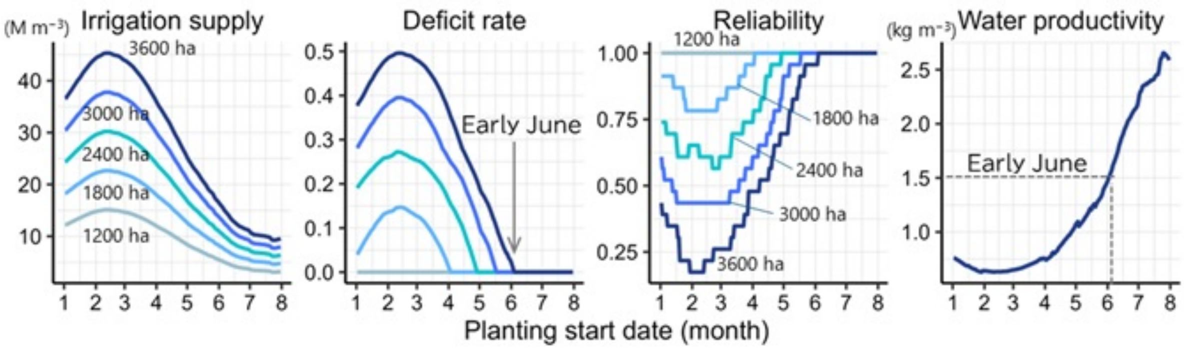

Fig. 2. Analysis of the impact of planting areas and timings on irrigation supply, deficit rate, reliability, and water productivity in single rice cropping

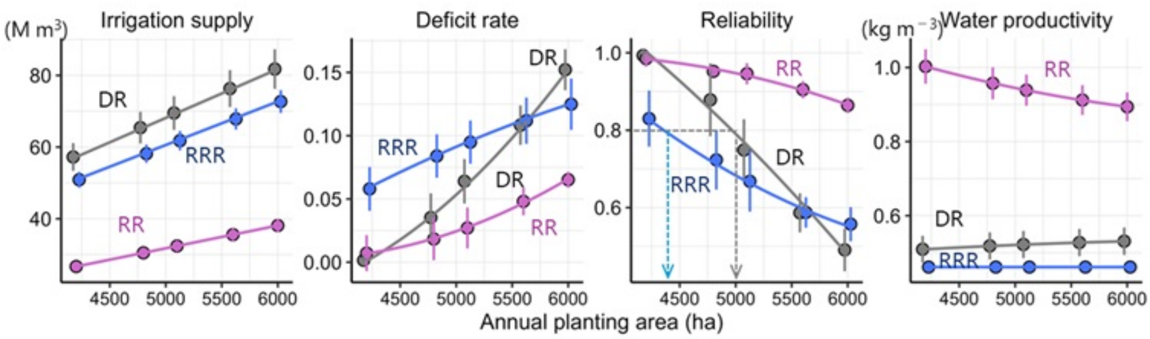

Fig. 3. Assessment of different planting areas on irrigation supply, storage deficit, deficit rate, and reliability in DR, RR, and RRR

DR, double rice-rice cropping; RR, double rice-ratoon cropping; RRR, triple rice-ratoon-ratoon cropping. Vertical bars across lines represent standard deviations.

Reference: Shiraki et al. (2025) *Agricultural Water Management* 307: 109251.

BNI-enabled sorghum reduces fertilizer application in India

Fertilizer consumption in India increased after the 'Green Revolution' and was the second highest in the world in 2018; furthermore, it has been strengthened by fertilization subsidies. Excessive subsidies, especially for urea, have distorted the balanced application of fertilizers, degraded the environment, and increased stress on national finances.

Biological nitrification inhibition (BNI) from plant root systems effectively curtails nitrogen (N) loss and enhances N utilization efficiency. BNI is increasingly important as a technology for mitigating greenhouse gas (GHG) emissions and water pollution, especially in countries where N fertilizer is overdosed.

This study aims to show the potential impacts of BNI-enabled sorghum varieties with a 30% soil nitrification inhibition rate on N fertilizer use, yield, life cycle GHG (LC-GHG) emissions, farmers' benefit, and government expenditure on subsidy under two scenarios: N fertilizer consumption is reduced (Scenario 1) or maintained (Scenario 2). We analyzed the farm survey data collected in Maharashtra, India, a major sorghum-growing state, for Rabi (in 2020–2021, n = 250) and Kharif sorghum (in 2022, n = 209). LC-GHG emissions were calculated using the life cycle assessment method (Fig.1).

Under Scenario 1 (Fig. 2, left), compared with conventional sorghum, the introduction of BNI-enabled sorghum reduced N fertilizer application in the Rabi and Kharif seasons by 8.0% and 7.4%, respectively. It also decreased area-scaled/yield-scaled LC-GHG emissions by 15.6% in the Rabi season and 11.2% in the Kharif season, while slightly increasing farmers' benefits. These changes could decrease the government's expenditure on urea fertilizer subsidies by 9.1%. However, many farmers indicated that they would not change the N fertilizer application even if the yield per N fertilizer application increased. Even under these circumstances (Scenario 2, Fig. 2, right), compared with conventional sorghum, area-scaled/yield-scaled LC-GHG emissions were decreased by 11.3% and 13.5% in the Rabi season and 8.1% and 10.2% in the Kharif season, respectively. Yield and farmers' benefits would increase by 2.5% and 4.9% in the Rabi season and by 2.4% and 6.5% in the Kharif season, respectively, but the government's expenditure on fertilizer would remain unchanged.

These results indicate that BNI-enabled sorghum can be used in two ways: reduced N fertilizer consumption (Fig. 2, left) or maintained consumption (Fig. 2, right). Some countries cannot apply enough N fertilizer to meet plant requirements, leading to low yields and exhaustion of soil fertility. BNI-enabled sorghum can be introduced in countries with low N fertilizer use to increase yield while maintaining fertilizer consumption, and in countries with high N fertilizer use to maintain yield while reducing fertilizer consumption.

Authors: Leon, A. [JIRCAS], Nedumaran, S. [ICRISAT]

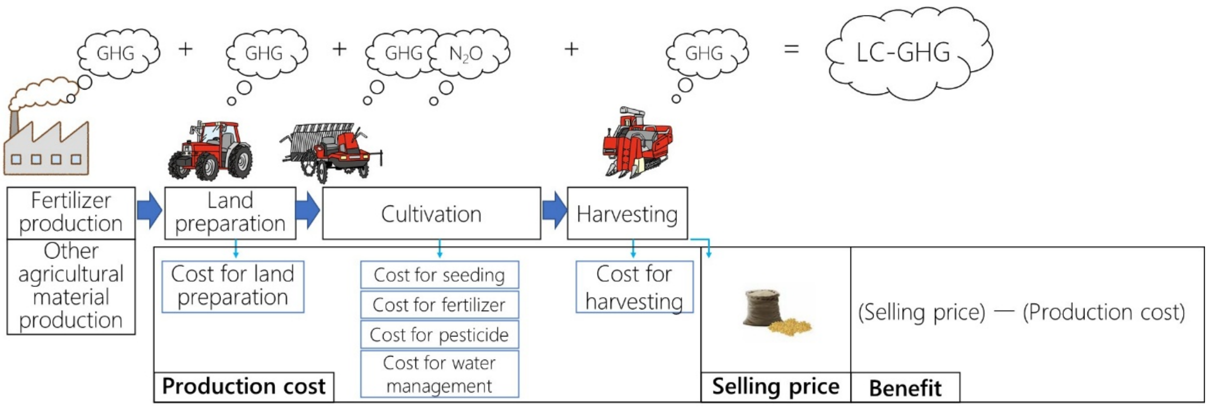

Fig. 1. Life cycle greenhouse gas (LC-GHG) emissions and benefits

LC-GHG is the sum of emissions from agricultural material production to harvesting.

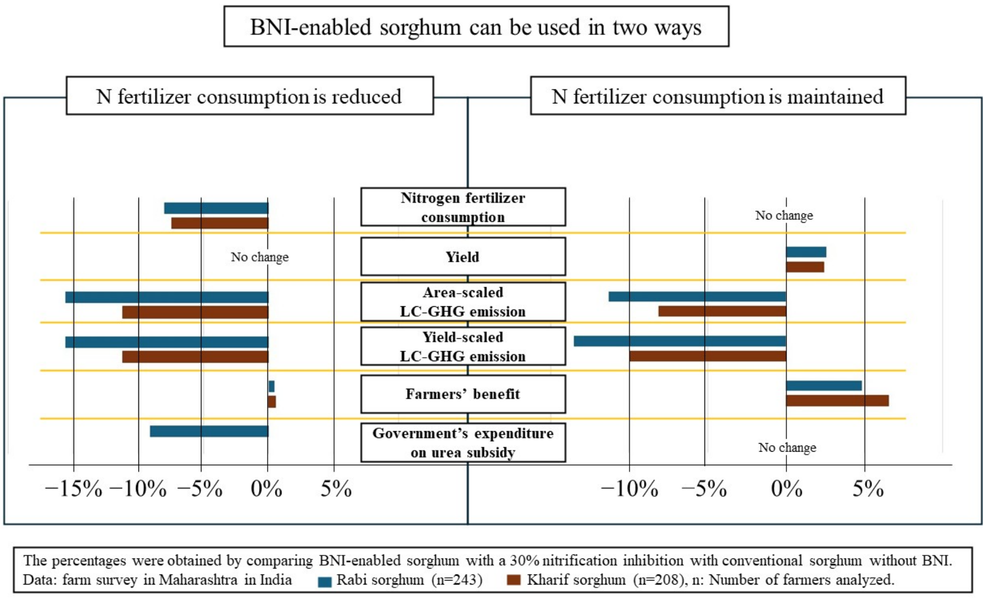

Fig. 2. The impact of BNI-enabled sorghum on nitrogen fertilizer consumption, yield, area-scaled/yield-scaled LC-GHG emissions, farmers' benefits, and the government's expenditure on urea subsidy when N is reduced (left) and maintained (right)

BNI-enabled sorghum could be a potential technology for establishing a sustainable agricultural system with the same yields (left) or higher yields (right) with lower GHG emissions and higher farmers' benefits.

Reference: Leon and Nedumaran. (2024) *Science of the Total Environment 957*: 177385.

Leaf chlorophyll content is an indicator of growth rate of tropical teak tree

Teak (*Tectona grandis*) is an important timber resource in tropical forests and has a high market value, so a stable supply is required. However, there are large differences in growth rates between individual trees even within the same teak plantation. This difference limits accurate prediction of future timber yields. Various leaf traits such as leaf size, nutrient, and pigment contents affect photosynthesis; thus, they are likely to be related to the tree growth rate. For example, chlorophyll is a pigment that absorbs the energy of sunlight for photosynthesis, and if it is lacking, the photosynthetic rate decreases and growth becomes restricted. If the difference in growth rates between individuals can be easily estimated from leaf traits, it will lead to improved accuracy in predicting yields and rapid identification of areas of poor growth. This study examines the relationship between growth rate and leaf traits related to photosynthesis in teak trees.

We measured the height and diameter of teak trees in four plantation forests aged 14 to 46 years old in Malaysia and found a large variation in diameter and height within plantations (Fig. 1). Canopy leaves were collected and compared for leaf area, chlorophyll content indexed by SPAD value (hereafter referred to as chlorophyll content), nitrogen content, and leaf mass per area. Leaf traits vary greatly among individuals even within the same plantation, and they also differ in appearance (Fig. 2). Leaf chlorophyll content positively correlates with diameter and height growth rates, suggesting that individuals with high chlorophyll content also have high growth rates (Fig. 3). In contrast, there is no correlation between other leaf traits and tree growth (Table 1).

Using leaf chlorophyll content as an indicator of growth, this approach can be used to improve the accuracy of timber production across large plantation areas using remote sensing technology such as drones and satellites, and also contribute to identifying areas of poor growth in the plantation. Although these results were obtained from teak plantations in Malaysia, confirming whether similar results can be obtained from teak plantations in other regions with significantly different climates and soil traits, as well as to teak varieties that differ genetically, could make these findings useful for forest tree breeding.

Authors: Tanaka, K. [JIRCAS], Yoneda, R., [FFPRI], Azani, M.A. [Univ. Malaysia Putra]

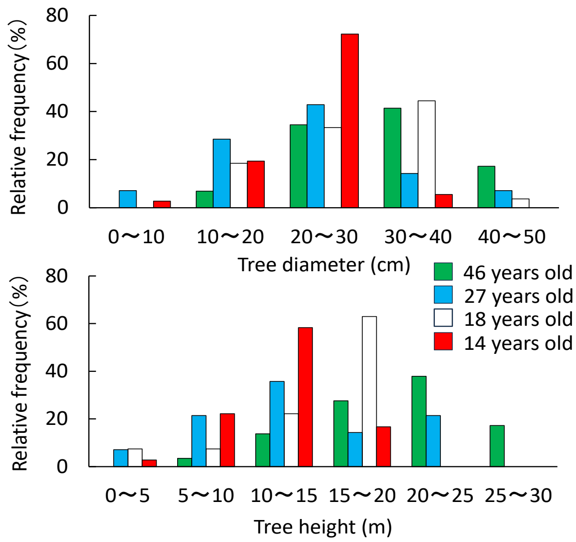

Fig. 1. Frequency distribution of tree height and diameter

Bar colors indicate plantation age.

Fig. 2. Leaves taken from same plantation

Each leaf is from a different individual. Dark green leaves contain a high amount of chlorophyll.

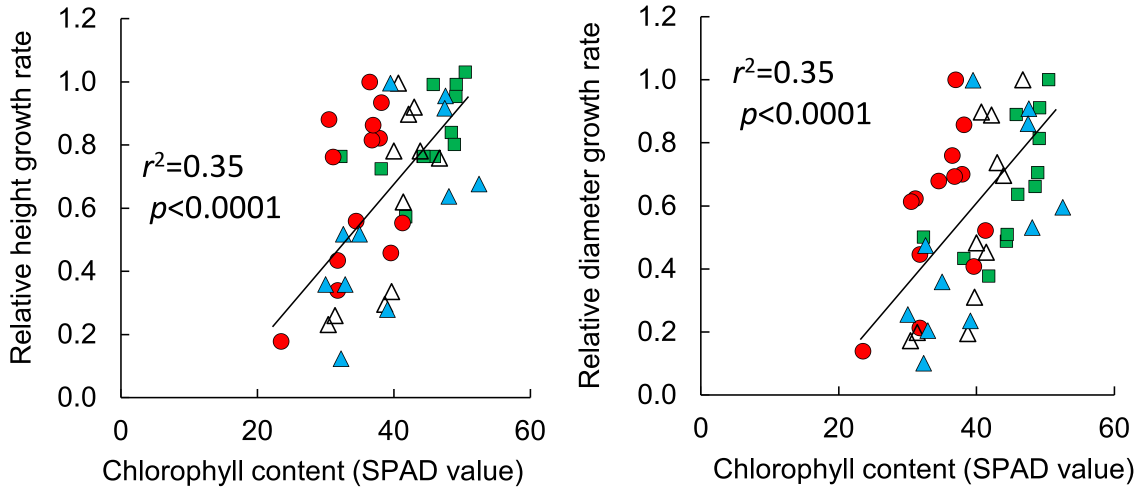

Fig. 3. Relationship between chlorophyll content and tree height (left) and diameter (right) growth

The symbol colors indicate stand age as in Fig.1, and the solid line represents the regression line.

Table 1. Results of multiple regression analysis of leaf traits and height and diameter growth rates in teak trees

Explanatory variables for growth rate	Relative height growth rate	Relative diameter growth rate
Nitrogen content	0.177	0.184
Chlorophyll content (SPAD value)	0.475**	0.561**
Leaf area	0.249	0.174
Leaf mass per area	−0.044	−0.001
Stand age	0.057	−0.153

The values are standardized coefficients, and ** indicates a significance level of p<0.01.

Predicting responses to soil desiccation from leaf traits in potted saplings among Dipterocarpaceae species

Ever-wet tropical forests of Southeast Asia account for a large fraction of forestry production in the world, but there are increasing concerns that this productivity will decline due to increased intensity and frequency of droughts associated with climate change. Hence, there is an urgent need to implement climate change adaptation measures by improving the drought tolerance of plantation trees. The Dipterocarpaceae, an important timber resource in this region, consists of >470 species, and there are potentially useful species with high drought tolerance. However, the drought tolerance of individual species and its indicators are unknown, which poses a challenge in implementing climate change adaptation through conversion of planting species.

This study aims to evaluate interspecific differences in drought responses and to identify traits which predict species' drought response through soil desiccation experiments on potted saplings of eight dipterocarp species, which differ in their distributions and morphological characteristics.

We artificially dried the soil of pots by stopping irrigation in a growth chamber with controlled environments and monitored the changes in physiological and morphological traits related to drought survival (leaf photosynthesis and degree of wilting) to quantify the drought response of each species (Fig. 1). We found that, regardless of species, stomatal conductance decreased at the earliest stage of soil desiccation, followed by a decrease in electron transport rate. The decline in maximum quantum efficiency and leaf wilting occurred at approximately the same time under severely dehydrated soils (Table 1). There were interspecific differences in the response of stomatal conductance, electron transport rate, and wilting progression to soil desiccation (Table 1). These species' drought responses were significantly associated with leaf-level drought-avoidance capacity, such that species with drought-avoidant leaves can maintain photosynthetic metabolism and avoid wilting under strongly desiccated soils (Fig. 2).

Overall, leaf drought-avoidance capacity is a convenient indicator of drought response in potted saplings of dipterocarps species and can be used to efficiently search for species with high drought tolerance. However, it should be noted that the above results were obtained from young potted saplings under controlled temperature, humidity, and light conditions and need to be validated in plantations and mature trees, where these environmental conditions vary over time and space.

Authors: Kawai, K. [JIRCAS], Ng, K.K.S., Lee, S.L. [Forest Research Institute Malaysia (FRIM)]

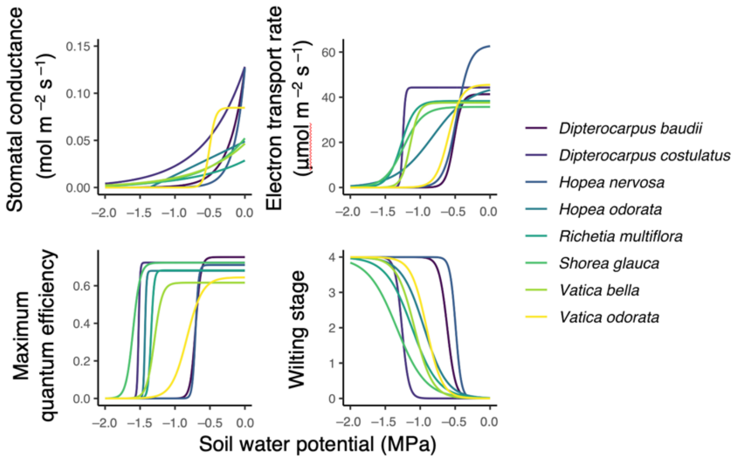

Fig. 1. Decline of photosynthesis and progression of wilting against soil desiccation

Higher absolute values in soil water potential indicate higher drought stress. Higher stomatal conductance and electron transport rate indicate higher photosynthetic rate. Lower maximum quantum efficiency indicates that more photosynthetic apparatus is damaged. Higher wilting stages indicate that wilting is more progressed. Different colors indicate different species.

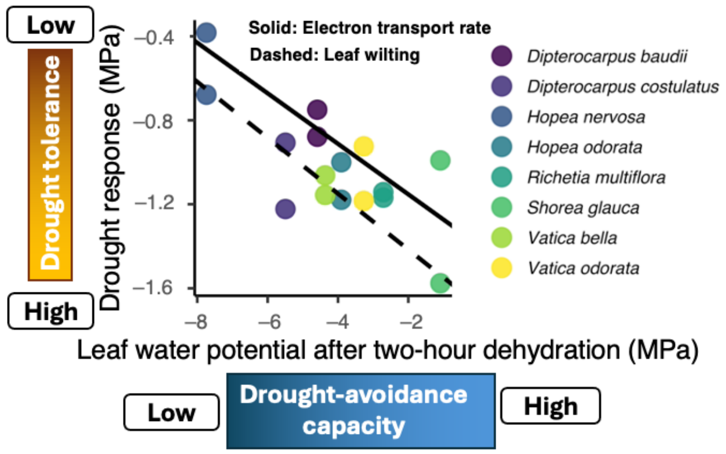

Fig. 2. Relationship between drought response and drought avoidance capacity at the leaf level

Higher absolute values in drought response show that changes against soil desiccation are small and indicate high drought tolerance. Lower absolute values in leaf water potential after two-hour dehydration indicate lower drought stress experienced under desiccating conditions and higher drought-avoidance capacity. Solid and dashed lines indicate trends of electron transport rate and leaf wilting, respectively.

Table 1. Responses of leaf photosynthetic paraments and wilting stage to soil desiccation

Species	Leaf characteristics			
	Stomatal conductance	Electron transport rate	Maximum quantum efficiency	Leaf wilting
Dipterocarpus baudii	−0.21^{a}	−0.75^{ab}	−0.95	−0.88^{ab}
Dipterocarpus costulatus	−0.38^{ab}	−0.91^{ab}	−1.32	−1.22^{ab}
Hopea nervosa	−0.22^{ab}	−0.38^{a}	−0.84	−0.68^{a}
Hopea odorata	−0.67^{ab}	−1.00^{ab}	−1.34	−1.18^{ab}
Richetia multiflora	−0.26^{ab}	−1.14^{b}	−1.34	−1.17^{ab}
Shorea glauca	−0.25^{ab}	−0.99^{ab}	−1.54	−1.58^{b}
Vatica bella	−0.37^{ab}	−1.06^{b}	−1.26	−1.16^{ab}
Vatica odorata	−0.70^{b}	−0.92^{ab}	−1.04	−1.18^{ab}
Average	−0.38^{A}	−0.75^{B}	−0.95^{C}	−0.88^{C}

Units: MPa. Higher absolute values show that changes against soil desiccation are small and indicate high drought tolerance. Differences in lowercase alphabets show significant differences among species, whereas differences in uppercase show differences among leaf characteristics (p < 0.05, Tukey test).

Reference: Kawai et al. (2025) *Kanto Shinrin Kenkyu* 76(1): 81–84.

Biochar application to soil surface layer effectively reduces nitrogen leaching under crop-present conditions

The Haber–Bosch process enables humanity to produce nitrogen fertilizer, allowing the population to grow by increasing food production. However, nitrogen applied as fertilizer often leaches from farmland in nitrate form, moving into water bodies such as groundwater and rivers and polluting the surrounding environment. Therefore, mitigating nitrogen leaching is urgently required. Biochar has been applied to farmlands to mitigate leaching while storing carbon. The effect of biochar application differs depending on the application depth; however, the effect of the application depth has not been evaluated under crop-present conditions. This study aimed to evaluate the effects of different biochar application depths on nitrogen leaching under crop-present conditions.

We conducted a pipe experiment with a plant (NERICA4) using bagasse biochar (800°C) with four treatments (Fig. 1): no biochar application (control), surface application (0–5 cm), plow layer application (0–30 cm), and subsurface application (25–30 cm). The experiment was conducted in a glass room. The amount of applied biochar was the same among the treatments (10 t ha^{-1}). Surface irrigation was conducted every two or three days, and powdered fertilizer was applied monthly. We measured the amount of nitrate and ammonium leaching during the experiment. Nitrate leaching was reduced by 12.3% by surface application ($p<0.05$), whereas nitrate and ammonium leaching were increased by 6.4% ($p<0.05$) and 164.1% ($p<0.01$) by plow layer application (Fig. 2). The subsurface application did not alter the leaching. We estimated the soil's dry condition and found that it was weaker at a depth of 10 cm under surface application, whereas it was stronger under plow layer application (Fig. 3, left). The root length density was increased at all depths under surface application, while it was smaller at the soil surface layer under plow layer application compared to the control (Fig. 3, right). The estimated amount of adsorbed inorganic nitrogen indicated that 75% of nitrogen existed at depths of 0–30 cm under surface application, whereas more than half of it existed at depths of 30–95 cm under plow layer application (Table 1).

Our study indicated that surface application reduced nitrate leaching; the reduction in soil's dry condition and the increase in adsorbed inorganic nitrogen might explain these differences. Choosing a proper biochar application depth could contribute to mitigating nitrate leaching and possibly reducing nitrogen fertilizer use.

Authors: Hamada, K., Nakamura, S., Kuniyoshi, D. [JIRCAS]

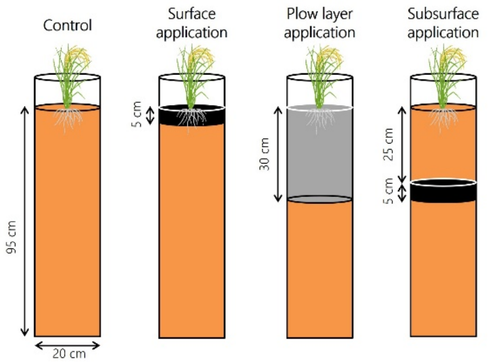

Fig. 1. Schematic of the experimental pipes
We applied four treatments with five replicates. The amount of applied biochar was the same among the treatments, but its content rate was different. Black and grey indicate high and low biochar content, respectively.

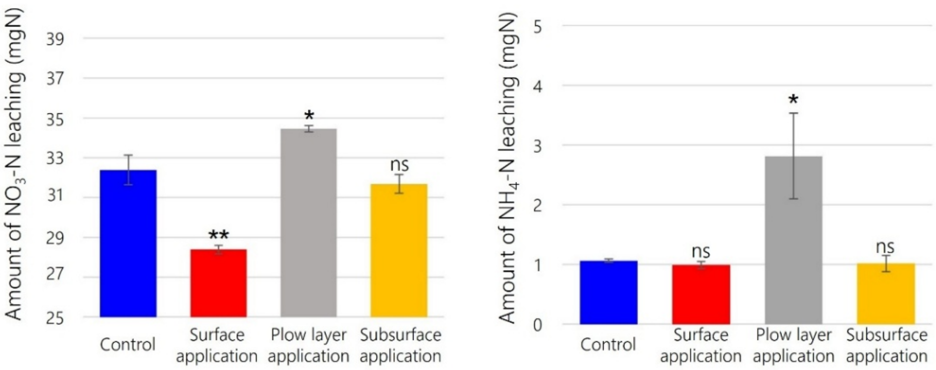

Fig. 2. Cumulative leaching amount of nitrate (left) and ammonium (right)
** and * indicate significant differences (p<0.01 and p<0.05), while ns indicates a non-significant difference compared with the control. Error bars represent the standard error.

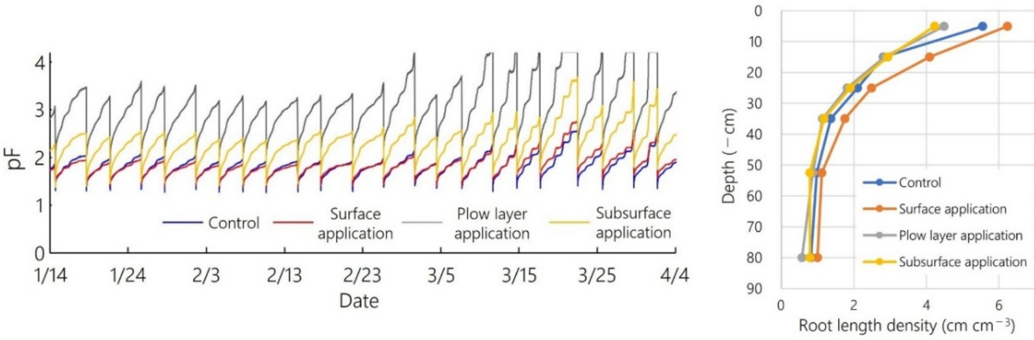

Fig. 3. Temporal change in pF (left) and distribution of root length density (right)
At pF>3, soil dryness increases, and water and nutrient absorption by roots decreases.

Table 1. Nutrient budget of inorganic nitrogen

	Control	Surface application	Plow layer application	Subsurface application
Inorganic nitrogen in soil (mg)				
0–30 cm depth				
Total	87	161	126	116
NO_3–N	17	31	12	19
NH_4–N	70	131	114	97
30–95 cm depth				
Total	27	25	38	25
NO_3–N	17	9	18	13
NH_4–N	10	16	20	12

Reference: Hamada et al. (2024) *Scientific Reports* 14: 22823.

Improving airborne LiDAR-based mangrove aboveground biomass estimation in the Philippines

Monitoring mangrove biomass is crucial for evaluating carbon storage, understanding carbon cycles, and studying climate change. Traditional estimation methods often underestimate biomass due to regional variations in species composition and tree height. LiDAR technology, which measures distances and shapes using laser light, allows for non-destructive, extensive biomass estimation. The study aimed to develop a biomass estimation formula for old-growth mangrove forests in the Philippines using national-level airborne LiDAR data and focused on improving the accuracy of biomass estimation models.

The Lorey's mean canopy height (H_m) and LiDAR relative height (*RH*) metrics were calculated for the old-growth mangrove forest in the Katunggan It Ibajay Ecopark (KII Ecopark) on Panay Island, Philippines (Fig. 1). The *RH* metrics were used to estimate H_m and above-ground biomass. Using the *RH* metrics, aboveground biomass was estimated in two ways: (i) Conventional method: Using the optimal *RH*, H_m was estimated, and then aboveground biomass was estimated using an existing formula (Suwa et al. 2021), and (ii) Developed equation: The newly developed equation directly estimates aboveground biomass using the optimal *RH* metrics. The relationship between H_m and the *RH* was verified, and then the conventional formula (above-ground biomass = $2.25H_m^{1.81}$ (Eq. 3) was applied to estimate above-ground biomass. The relative height at the 95th percentile (RH_{95}) corresponded best with H_m (R^2 = 0.79). When RH_{95} was applied to Eq. 3, above-ground biomass was underestimated in plots with high canopy height (R^2 = 0.46) (Fig. 2, left). The formula for estimating above-ground biomass using RH_{95} showed relatively high accuracy (Fig. 2, right: above-ground biomass = $0.02{*}RH_{95}^{3.56}$ (Eq. 4), R^2 = 0.58). The above-ground biomass map of the old-growth mangrove forest in KII Ecopark can be obtained using the developed Formula 4 (Fig. 3).

The newly developed equation is expected to enhance biomass measurement in old-growth mangrove forests, enabling extensive and correct assessments using airborne LiDAR data. This can contribute to measurement, reporting, and verification (MRV) processes, although incorporating additional variables, such as tree diameter, could further improve accuracy. The study highlights the importance of advanced methods for better understanding and managing mangrove ecosystems in the context of carbon storage and climate change.

Authors: Mandal, M.S.H., Suwa, R. [JIRCAS], Rollon, R.N., Albano, G.M.G., Cruz, A.A.A. [Univ. of the Philippines], Ono, K. [FFPRI], Primavera-Triol, Y.H. [Aklan State Univ.], Blanco, A.C. [Univ. of the Philippines], Nadaoka, K. [Tokyo Tech.; Kajima Tech. Res. Inst.]

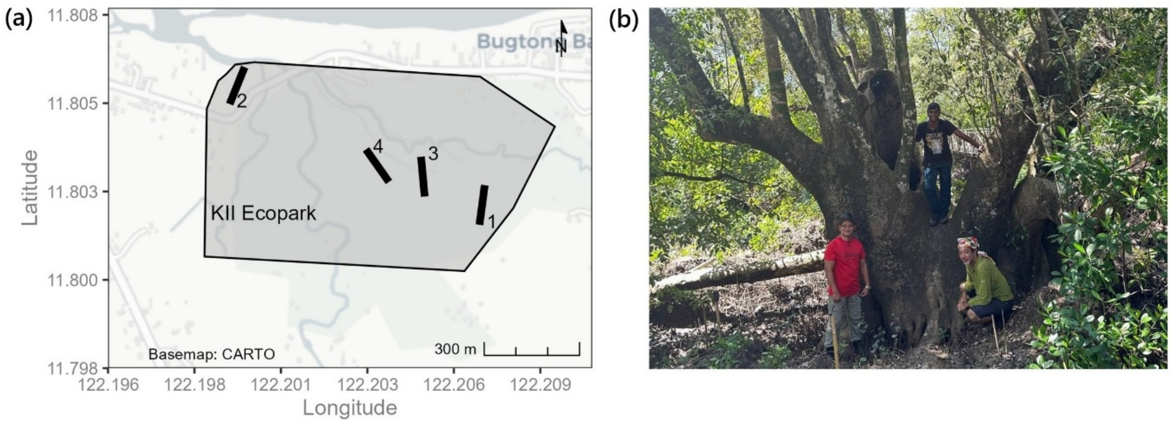

Figure 1. Katunggan It Ibajay Ecopark (KII Ecopark) on Panay Island, Philippines

(a) The location of the survey area and the transect plots (▮), with the numbers indicating the survey transect ID. (b) A very old *Avicennia rumphiana* tree in the survey area

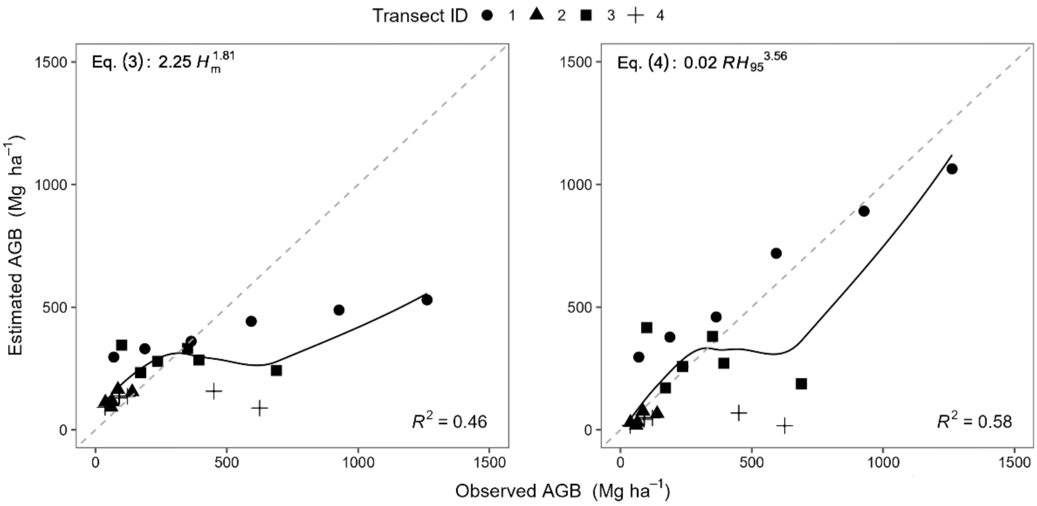

Figure 2. Relationship between observed aboveground biomass (AGB) and estimated aboveground biomass (AGB) using Eq. (3) (left) and Eq. (4) (right)

The dashed line indicates a 1:1 ratio. The solid line indicates a trend based on the Loess method.

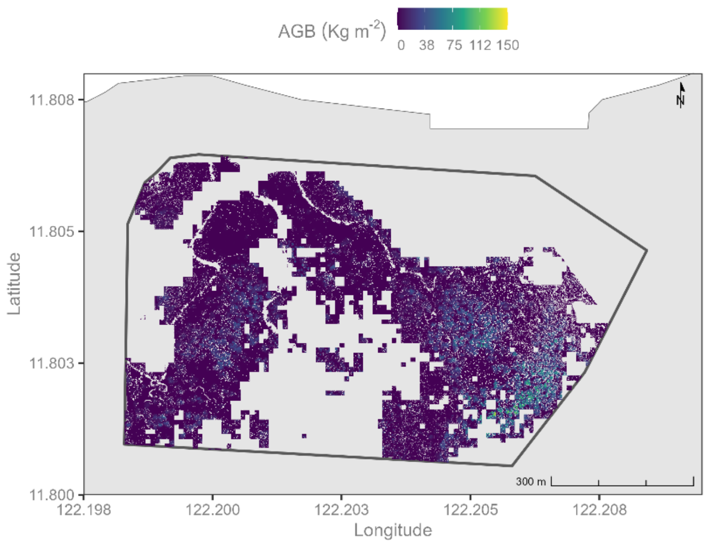

Figure 3. Aboveground biomass (AGB, kg m^{-2}) map in the KII Ecopark

Reference: Mandal et al. (2024) *Ecological Research* 40: 120–132.

The effect of improving soil salinity and pH by Cut-soilers (shallow sub-surface drainage) is high at a construction spacing of 2.5 m

In the Indo-Gangetic Plain (IGP), salinization due to irrigation with highly saline groundwater and poor drainage in the field has been a serious problem. In addition, soil sodicity, which increases the proportion of sodium ions, is occurring. Specifically, poor drainage due to sub-surface soil sodicity is worsening. Constructing sub-surface drainage is effective in mitigating salinization, but it is difficult for farmers to implement due to substantial costs. The Cut-soiler, a tractor attachment developed in Japan, can construct shallow sub-surface drainage (40–60 cm depth) while burying crop residues and/or soil improvement agents simply by towing it with a tractor (Fig. 1) (2022 JIRCAS Research Highlights: Shallow sub-surface drainage constructed with "Cut-soiler" mitigates soil salinity). Therefore, this technology could be a sustainable countermeasure against salinization for farmers in developing countries because it is inexpensive and easy to use.

In this study, we investigated the optimal construction spacing (2.5, 5, 7.5, 10 m) that achieved the highest effectiveness with this shallow sub-surface drainage in the salinized area of the IGP. Additionally, we implemented an effective measure to address soil sodicity by applying gypsum ($CaSO_4$) at 10 t ha^{-1}. This treatment replaces the sodium ions with calcium ions, promoting the leaching of sodium. Simultaneously, we buried rice straw at 6 t ha^{-1} using this technology and verified the reduction effect in soil pH. Comparing the spacings, the reduction in soil salinity (EC_e) after 3 years of construction was highest at 2.5 m spacing (Fig. 2), and the yield of rainy season crops (pearl millet) was also highest at 2.5 m spacing (Fig. 3). On the other hand, comparing the soil pH, the reduction in soil pH after 2 years of construction was highest at the 2.5 m spacing (Fig. 4). Furthermore, the reduction in soil pH was higher the closer to the Cut-soiler construction line (Fig. 5).

This technology can be widely applied to similar salinized areas because it can be easily implemented using a tractor. To extend this method widely, a "Technical manual" focusing on shallow sub-surface drainage with Cut-soiler will be compiled. In India, this technology will be disseminated through the Indian Council of Agricultural Research (ICAR) and the Central Soil Salinity Research Institute (CSSRI). Since the construction method of shallow sub-surface drainage with Cut-soiler varies depending on the drainage situation around the field, it is necessary to check the drainage conditions in advance. The Cut-soiler is not equipped with wheels for transportation. The expected useful life of the Cut-soiler is approximately 7 years when constructing 30–50 ha per year. If there is no damage to the frame, it can be used continuously by replacing consumables.

Authors: Yadav, G., Yadav, R. K., Rai, A. K., Kumar, S., Neha [CSSRI],
Onishi, J., Kameoka, T., Matsui, K., Lee, G. [JIRCAS], Kitagawa, I. [NARO]

Fig. 1. (a) Cut-soiler, (b) Construction with Cut-soiler, and (c) Schematic diagram

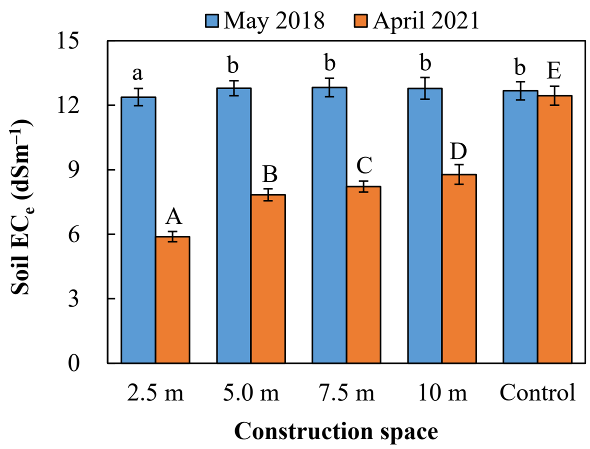

Fig. 2. Change in soil salinity
The sub-surface drainage was constructed with Cut-soiler in May 2018. There are significant differences (at the 1% level) between different symbols. Error bars are standard deviations (n=108).

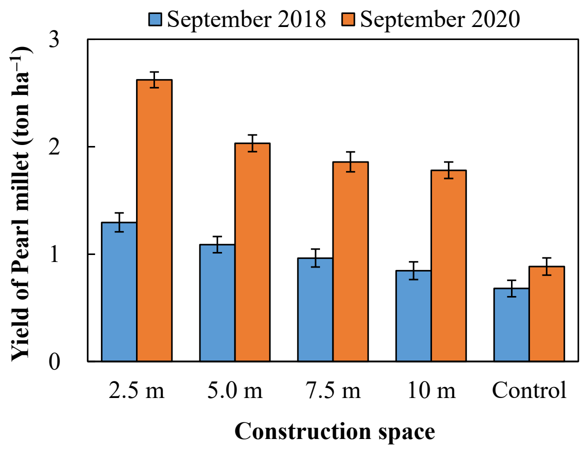

Fig. 3. Yield of pearl millet
The sub-surface drainage was constructed with Cut-soiler in May 2018. There are significant differences (at the 1% level) between different symbols. Error bars are standard deviations (n=9).

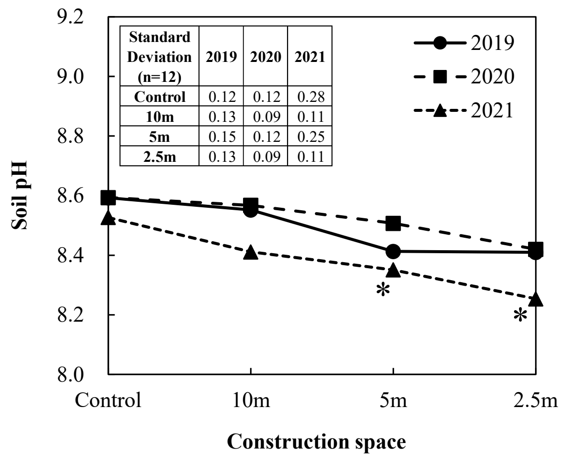

Fig. 4. Soil pH at each spacing
The sub-surface drainage was constructed with Cut-soiler in July 2019. * indicates significant difference (at the 5% level) from Control, 2019.

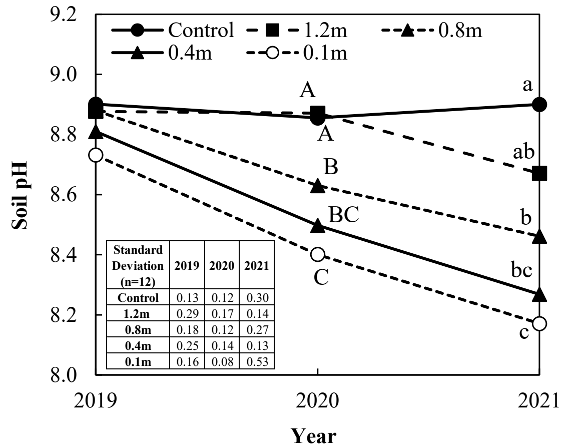

Fig. 5. Soil pH at each distance
The sub-surface drainage was constructed with Cut-soiler in July 2019. There are significant differences (at the 5% level) between different symbols.

References: Gajender, Y. et al. (2024) *Journal of Arid Land Studies* 34(S), 21–24;
Rajender, K.Y. et al. (2024) *Journal of Arid Land Studies* 34(S), 29–32.

Changes in location and structure of underground pipes enhance water vapor collection in plastic film tunnels

Agriculture is the largest water user, with 70% of the world's freshwater withdrawn for irrigation. Ishikawa et al. (1996) developed an "earth-air heat exchange water distillation system" that can produce freshwater by collecting water vapor in a plastic film tunnel as condensed water on the insides of the plastic film and underground pipes. Their system successfully collected 30% of the evaporated water. This study aimed to develop a simple water distillation system constructed from agricultural materials, suitable for installation in rural areas, while improving the earth-air heat exchange water distillation system to enhance water vapor collection.

Three plastic film tunnels (1.2 m wide, 0.6 m high, 8.0 m long) were built, and three types of underground pipes were embedded at 20 cm depth below ground: i) one PVC pipe with a diameter of 100 mm below the tunnel (control; Ishikawa model), ii) one PVC pipe with a diameter of 100 mm outside the tunnel (100 mm outer), and iii) four PVC pipes with diameters of 50 mm outside the tunnel (50 mm x 4 outer). Different underground pipes were selected for each tunnel and rotated for the next trials. Water tubs serving as evaporation pools were put in the tunnels, and the water in the pools was heated by solar radiation and evaporated. Hot and humid air was blown into the pipes by a fan with a solar panel, and water vapor was cooled by soil temperature around the underground pipes and condensed on the inside of the pipes. The water vapor in the tunnel was cooled by ambient air, and condensed water on the inside of the plastic film was collected by L-shaped aluminum frames placed under the plastic film on both sides of the tunnel. The collected freshwater was stored in tanks at the tail end of the tunnel (Figs. 1 and 2).

Soil temperature at the ground surface, pipe wall temperature, and air temperature in the pipes embedded outside the tunnel tended to be lower than those of the control. In particular, the pipe wall temperature of 50 mm x 4 outer was significantly lower than the control (Table 1). In the case of 50 mm x 4 outer, 12.4 L of freshwater was produced from one tunnel on a sunny day in March in Tsukuba, Ibaraki, Japan. The water vapor collection ratio, defined as the ratio of collected water volume to evaporated water volume, for the pipes of the control, 100 mm outer, and 50 mm x 4 outer was 4.3%, 11.3%, and 23.3%, respectively (shown as the orange color bar in Fig. 3). The water vapor collection ratios for the plastic films were 30.3% using the control, 27.2% using 100 mm outer, and 22.5% using 50 mm x 4 outer (shown as the blue color bar in Fig. 3). The total collection ratio for both the pipes and plastic film of 50 mm x 4 outer was 46%, which was 1.3- and 1.2-times higher compared to the control and 100 mm outer, respectively.

Authors: Ikeura, H. [JIRCAS], Fujimaki, H. [Tottori Univ.]

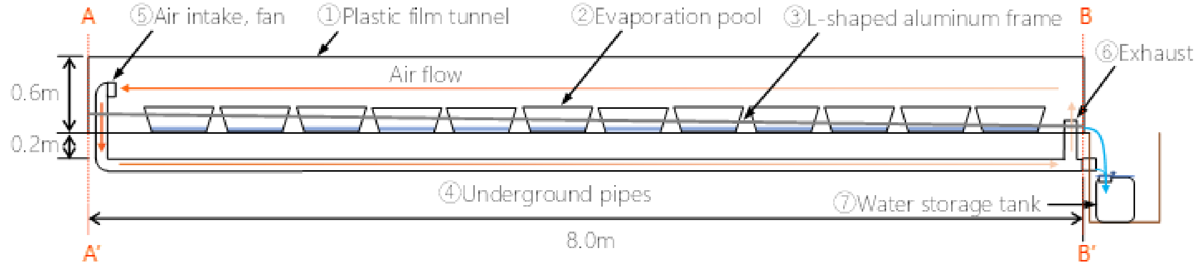

Fig. 1. Schematic of the improved earth-air heat exchange water distillation system
Sectional notations are shown as A-A', B-B', and the numbers ①-⑤ are common items with Fig. 2.

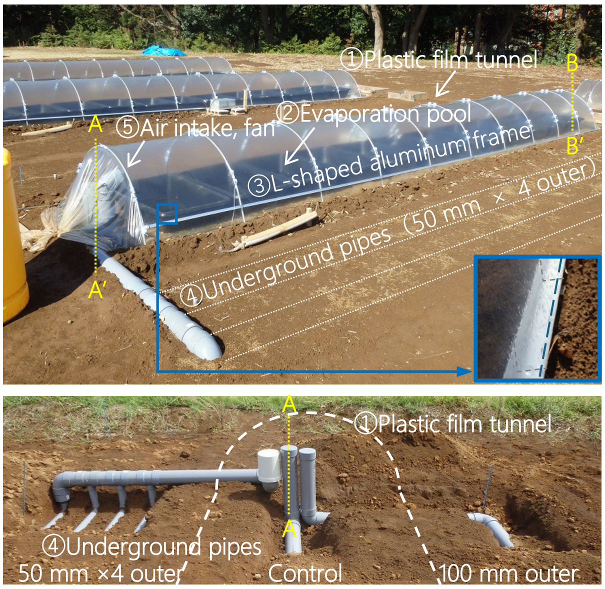

Fig. 2. Plastic film tunnel and underground pipes
Upper photo shows the structures above ground, with the blue line box showing an enlarged view of the L-shaped frame. The frame ridge, shown as a blue dashed line, is adhered to the inside of the plastic film. Lower photo shows the pipes buried underground.
Sectional notations shown as A-A', B-B' and the numbers ① -⑤ are common items with Fig. 1.

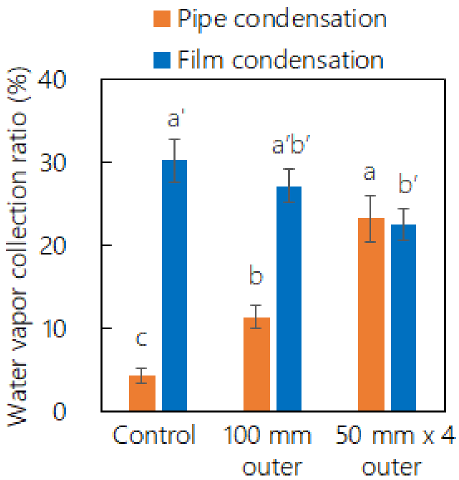

Fig. 3. Water vapor collection ratio by underground pipes and plastic film
Error bars show standard error (n=12). Significant differences were found among a-b-c and a'-b' (p < 0.05, Tukey Kramer HSD test).
Water vapor collection ratio
= collected water volume
/ evaporated water volume.

Table 1. Daily average temperatures of the air in the tunnel, soil, inner wall, and inner air of the underground pipes

	Air temp. in the tunnel (°C)	Soil temp. at ground surface (°C)	Soil temp. at 10-cm depth (°C)	Pipe wall temp. at 20-cm depth (°C)	Air temp. in the pipes (°C)
Control	19.8	19.3[a]	20.4[a]	22.2[a]	22.9[a]
100 mm outer	19.5	12.6*	14.5[b]	19.0[ab]	19.9[ab]
50 mm × 4 outer	19.2	11.9[b]	14.6[b]	18.3[b]	19.1[b]

n = 12 (*Lacking 4 ground surface data points for 100 mm outer.)
Significant differences were found between a and b (p < 0.05, Tukey-Kramer HSD test)

Reference: Ikeura and Fujimaki (2024) *Paddy and Water Environment* 23: 95-109.

Development of a cryogen-free extraction and preservation method for plant-derived RNA

Increasing the resilience of plants to environmental stress is crucial for improving crop yield. Understanding gene expression patterns provides insight into stress tolerance mechanisms and accelerates the development of high-performance crops. RNA used for gene expression analysis is unstable, and its analysis usually requires cryogens such as liquid nitrogen and dry ice. Thus, gene expression analysis in samples from developing countries with limited access to cryogens has been challenging. While companies have released RNA preservation reagents that maintain the quality of RNA in living organisms without cryogens, the effects of different sample storage conditions on overall gene expression patterns and the optimal storage conditions for maximizing RNA stability in plants have not been thoroughly investigated. In addition, the long-distance transport of extracted RNA without cryogens has also been a hurdle. Considering the application in developing countries, this study aimed to establish cryogen-free methods to transport 1) high-quality plant leaf specimens from the field to the laboratory for gene expression analysis, and 2) isolated RNA for genomics analysis.

In the newly developed "infiltration method," a commercial RNA preservation reagent is infiltrated into the apoplast (intercellular space) of a plant leaf using a syringe (Fig. 1). When comparing the expression patterns in rice leaf samples treated with the infiltration method to those simply immersed in the solution (both stored at 4°C for 5 days), the former better preserved the original RNA expression pattern obtained by freezing samples with liquid nitrogen (Fig. 2). The effectiveness of the developed infiltration method was validated in Madagascar by demonstrating that leaf samples from fields with poor plant growth exhibited significantly higher expression of phosphorus deficiency- or iron deficiency-inducible genes (Fig. 3). Thus, the use of the infiltration method allowed for detection of nutrient disorders even without the use of cryogens in a developing country. Additionally, it was found that the extracted RNA remained relatively stable (for 48 hours) when bound to a silica-based membrane compared to being in a solution (Fig. 4).

One limitation is that the infiltration method may bias salinity- or cold stress-related genes compared to freezing with liquid nitrogen, and caution should be taken when analyzing such stresses using the infiltration method. Nevertheless, the application of the infiltration method is expected to accelerate gene expression analyses in plant samples collected from fields in developing countries. The possibility of long-distance transport of RNA without cryogens offers the possibility to run genomics studies (e.g. RNA sequencing) using such samples.

Author: Ueda, Y. [JIRCAS]

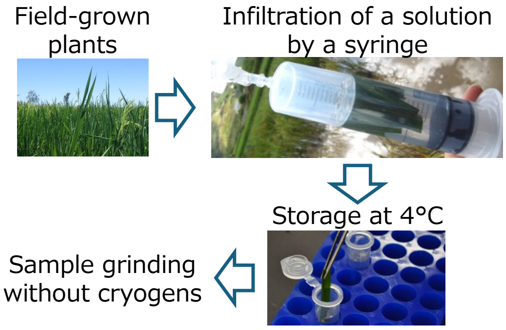

Fig. 1. Summary of the infiltration method
The leaf surface is washed briefly with a detergent solution and then infiltrated with a commercial RNA stabilization solution using a syringe. The samples are then stored at 4°C, allowing for RNA extraction without the need for cryogens.

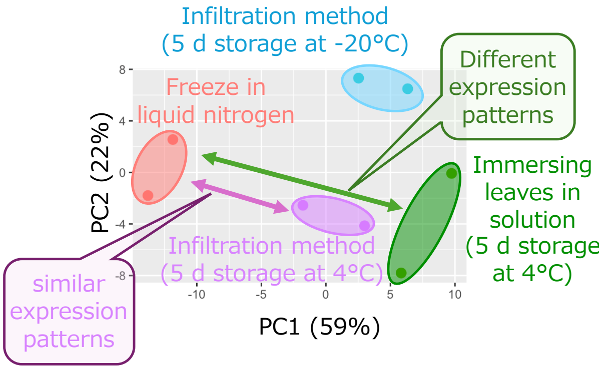

Fig. 2. Evaluation of the infiltration method through RNA sequencing
The results of principal component (PC) analysis using samples stored under different conditions are shown. Each dot represents a sample, with closely plotted samples indicating similar expression patterns. The data indicates that the infiltration method better preserves the original expression pattern compared to simply immersing leaves in the solution. In addition, the storage at 4°C is recommended over −20°C post-infiltration.

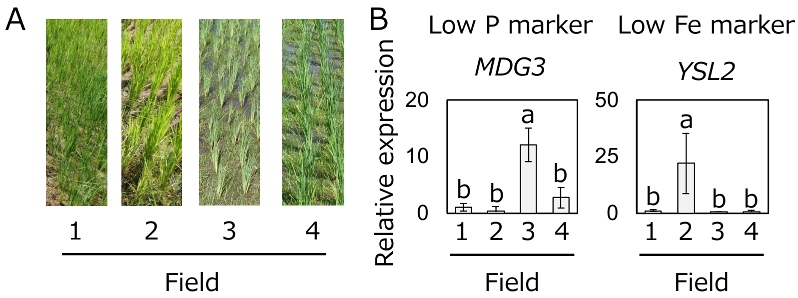

Fig. 3. Gene expression analysis using infiltration methods in Madagascar
A. The plants in 4 different fields from which leaves were harvested using the infiltration method. **B.** Expression of phosphorus (P) and iron (Fe) marker genes in the fields shown in A. Higher expression in each gene indicates that the plants suffer from a deficiency of each nutrient. Different letters indicate significant differences in expression (Tukey-Kramer post-hoc, $p < 0.05$). The data reveal that plants with pale-green leaves (field 2) and restricted tillering (field 3) suffer from P and Fe deficiencies, respectively.

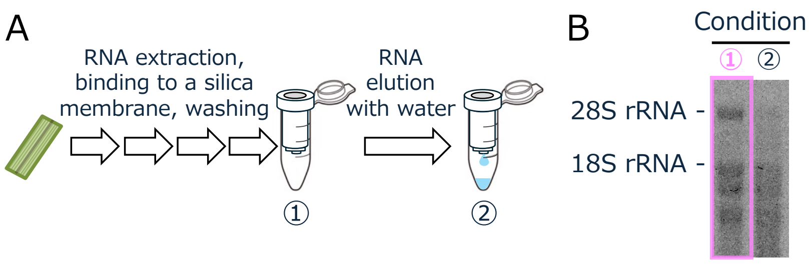

Fig. 4. Evaluation of different transportation methods for extracted RNA
A. The steps in RNA extraction. **B.** The results of electrophoresis using RNA samples bound on a silica membrane (①) and extracted with water (②) after a 48-hour transport from Madagascar to Japan on ice. Stronger bands of "28S" and "18S" rRNA, which indicate different sizes of ribosomal RNAs, suggest more intact RNA.

Reference: Ueda (2024) *Plant Methods* 20: 187.

Chromosome-level genome assemblies for highland quinoa cultivated in the Andean highlands

Quinoa is emerging as a key seed crop for global food security due to its ability to grow in marginal environments and its excellent nutritional properties. Our comprehensive genomic analyses revealed that the quinoa inbred lines can be categorized into three genetic sub-populations: the northern highland, southern highland, and lowland groups (2020 Research Highlights: Genetic and phenotypic variation of agronomic traits and salt tolerance among quinoa inbred lines). However, unlike lowland quinoa lines, no useful genomic information is available for highland quinoa lines. The high-quality genome assemblies obtained in this study will provide the basis for advancing functional genomics in quinoa to facilitate the development of climate-adapted highland quinoa breeding materials and contribute to a better understanding of the domestication process of quinoa, including its adaptation to harsh environments and its origin.

The whole genome sequences of J075 as a representative line of northern highland quinoa, and J100 as a representative line of southern highland quinoa were decoded using PacBio high-fidelity (HiFi) sequencing. Furthermore, we obtained their chromosome-level genome assemblies by integrating the HiFi sequencing reads and aligning them using the linkage map generated by dpMig-Seq. The assembled genomes of J075 and J100, each comprising 18 pseudochromosomes, exhibited sizes of 1.29 Gb and 1.32 Gb, with contig N50 values of 66.3 Mb and 12.6 Mb and scaffold N50 values of 71.2 Mb and 70.6 Mb, respectively, and were predicted to harbor 65,303 and 64,945 genes. As an example of comparative analysis of genome structure and diversity among quinoa genotypes, we selected genes homologous to the reported betalain biosynthetic gene sequences from each line and assessed genomic structural variation. Regions on chromosomes containing clusters of betalain synthesis genes *CqDODA1* and *CqCYP76AD1* were less conserved in genome structure compared to adjacent regions in each line, suggesting their association with the phenotypic differences between the dark-red highland and the light-colored lowland quinoa.

Detailed comparative analysis of genomes among representative quinoa genotypes is expected to facilitate the selection of crop design materials for developing quinoa varieties with enhanced stress tolerance, yield stability, and high nutritional value, which are critical for food security. These genomic data are publicly available via the Kazusa DNA Research Institute's "Plant GARDEN" portal.

Authors: Kobayashi, Y., Fujita, Y., Nagatoshi, Y., Fujii, K. [JIRCAS],
Hirakawa, H., Shirasawa, K. [Kazusa DNA Res. Inst.], Nishimura, K. [Okayama Univ.],
Oros, R. [PROINPA], Almanza, G.R. [Universidad Mayor de San Andres], Yasui, Y. [Kyoto Univ.]

Table 1. Genome assembly statistics of Northern and Southern highland quinoa lines

	Northern highland J075	Southern highland J100
Genome size (Gb)	1.29	1.32
Number of Genes	65,303	64,945
N50 (Mb) *	71.2	70.6
BUSCO (%)†	99.2	99.1
LAI score‡	17.40	17.75

*The N50 value is a statistical measure that reflects the contiguity and overall quality of an assembly. The higher the N50, the longer the average contiguous sequences in the assembly.

†The BUSCO measures genome assembly completeness by checking for the presence of essential, single-copy genes from the embryophyta dataset.

‡The LAI measures how effectively a genome assembly reconstructs LTR retrotransposons—higher scores reflect more complete and continuous assemblies of these repetitive regions.

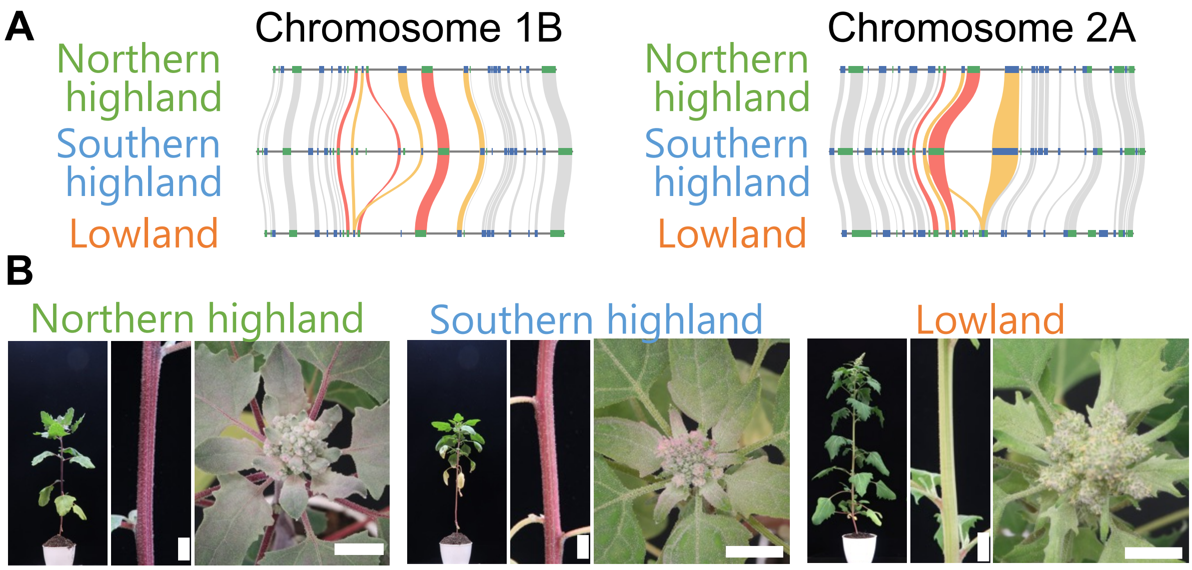

Fig. 1. Genomic structure of betalain biosynthesis gene clusters and plant color phenotypes in representative quinoa lines

(A) Structural conservation of the regions encompassing the betacyanin biosynthesis gene cluster on chromosomes 1B and 2A. The betalain biosynthesis genes, *CqDODA1* and *CqCYP76AD1*, are connected by red and orange lines, respectively, across quinoa genotypes.

(B) Phenotypes of stem and shoot apex colors in northern and southern highland and lowland inbred lines after 56 days of growth. Bars indicate 1 cm.

Reference: Kobayashi et al. (2024) *Frontiers in Plant Science* 15: 1434388. © The Author(s) 2024

The table and figure are modified from Kobayashi et al. (2024).

Enhancing yam yield through strategic planting: a climate-resilient approach

White Guinea yam (hereafter referred to as yam) is a major crop widely cultivated in the Guinea savanna region of West Africa, requiring 8 to 10 months from planting to harvest. The timing of the rainy season's onset and end is crucial for shoot growth and tuber enlargement. However, climate change is expected to shorten the rainy season in this region, potentially reducing yam yields by 33% by 2050. Adjusting the planting time of yam seed tubers has been proposed as a promising adaptation strategy, but its effectiveness remains unclear. Typically, yam is planted about one month after the rainy season starts to avoid drought stress during early growth. If climate change delays the onset of rainfall, postponing the planting period may cause the crop's late growth stages to coincide with the dry season, exposing it to drought stress and reducing yields. While *Dioscorea alata* (water yam) initiates tuber bulking based on photoperiod rather than planting date, little is known about the photoperiodic response of White Guinea yam. This study evaluates the impact of planting time on yam yield through on-farm trials in Nigeria, the world's largest yam-producing country.

Field trials examined three planting dates: early planting (at the beginning of the rainy season), normal planting (one month later), and late planting (two months later). The results showed that early planting led to harvest occurring about 90 days earlier than normal planting, with a 21% yield increase (Fig. 1). Tuber enlargement was determined by the number of days after planting rather than by calendar date, with minimal influence from photoperiod. Earlier planting advanced tuber bulking, allowing completion within the rainy season when soil moisture was sufficient (Fig. 2). The relatively low rainfall at the beginning of the rainy season had little effect on shoot growth or yield. In contrast, delayed planting caused tuber bulking to overlap with the dry season, significantly reducing yield due to drought stress. These findings highlight the risks associated with late planting under shifting rainfall patterns.

This study provides essential insights for optimizing yam cultivation systems under future climate conditions. Early planting can increase yield and mitigate the negative effects of rainfall variability, but some varieties exhibit unstable sprouting, necessitating the development of improved varieties and cultivation techniques. Additionally, extremely low rainfall at the beginning of the rainy season may delay shoot growth, increasing production risks. Further research is needed to refine planting strategies that ensure stable yields in response to changing climatic conditions.

Authors: Iseki, K. [JIRCAS], Olaleye, O., Matsumoto, R. [IITA]

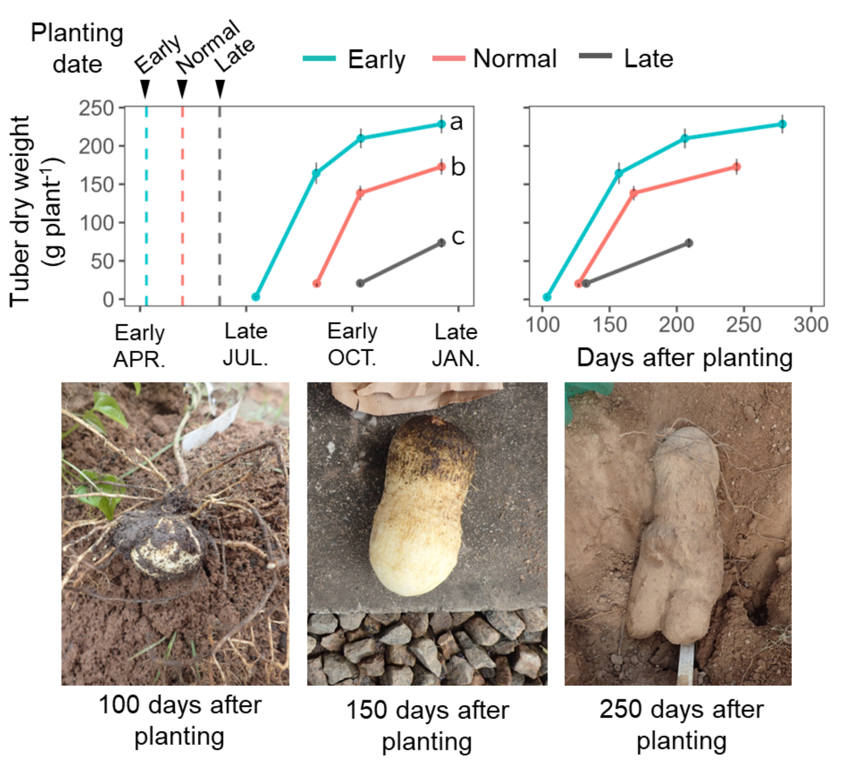

Fig. 1. Effect of planting time on tuber bulking growth

Data represent the average results from a two-year cultivation trial (2019–2020) conducted at the experimental field of the International Institute of Tropical Agriculture (IITA) in Nigeria, using two yam genotypes. Each sampling included four plants with three replications. Vertical bars indicate standard errors (n=48). The vertical lines in the figure represent planting dates. Different letters indicate significant differences in tuber yield at harvest ($p < 0.01$). The photos show representative tubers under normal planting conditions.

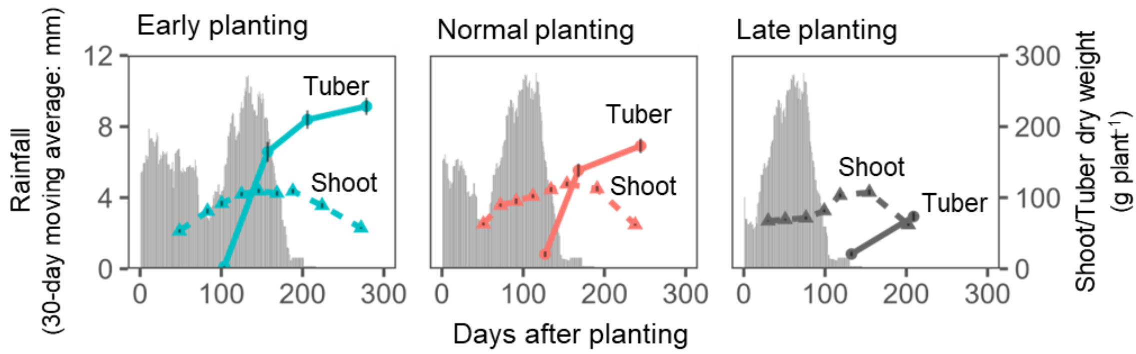

Fig. 2. Rainfall differences by planting time

The gray bars represent the 30-day moving average of rainfall over 300 days after planting, averaged over two years. The dashed line indicates changes in shoot dry weight, while the solid line represents changes in tuber dry weight (mean ± standard error, n=48). Early-season planting allows tuber bulking to be mostly completed within the rainy season. As planting is delayed, the amount of rainfall at the onset of tuber bulking decreases, leading to reduced tuber growth and a significant decline in yield.

Reference: Iseki et al. (2024) *Plant Production Science* 27: 212-220.

Organization and cost requirements of government-recommended fall armyworm control measures in Indochina countries

The fall armyworm (FAW), *Spodoptera frugiperda*, a polyphagous pest native to the Americas and known for causing significant damage to maize crops, was first detected in West Africa in 2016 and was reported in Southeast Asia by 2019. However, there is still room for a systematic organization of information on the FAW management strategies of ASEAN governments, including their feasibility for adoption at the farm level. This study categorizes FAW control measures recommended by governments and assesses their alignment with practices adopted by farmers in the Indochina region, including Myanmar, Thailand, Laos, Cambodia, and Vietnam. The findings aim to provide critical insights to support the development and dissemination of integrated pest management (IPM)-oriented FAW control technologies.

FAW control measures promoted by governments for farmers include brochures, websites, and social media in local languages. While many countries recommended chemical pesticides such as emamectin benzoate, concerns about resistance have led to the promotion of resistance management and biological controls, including microbial agents and natural enemies (Table 1). A survey of 127 feed maize farmers in Thailand in September 2021 revealed that foliar application of chemical pesticides was the dominant FAW control method, with no farmers reporting the use of seed treatments or natural enemies. From October 2022 to March 2023, interviews with 14 feed maize farmers in the Indochina region were conducted to analyze production costs for individual operations. Across various countries, pest prevention and control costs, including application and opportunity costs, accounted for less than 5% of total production costs for most farmers (Fig. 1). The foliar application of emamectin benzoate was prevalent, with material costs averaging \$9/ha and application costs \$5/ha, indicating relatively low expenses.

To encourage the adoption of chemical insecticide alternatives recommended by national governments, their costs must not become significantly higher than those of foliar applications of emamectin benzoate. According to our survey results and prior studies, seed treatments and the release of natural enemies show potential as cost-effective measures, warranting further investigation. However, the limited sample size of farmer interviews in this study highlights the need for broader surveys to draw more generalizable conclusions, particularly regarding specific figures such as the cost of emamectin benzoate.

Authors: Kusano, E., Kobori, Y. [JIRCAS]

Table 1. FAW control measures recommended by three or more Indochina countries

Method	Description	Country
Sampling and monitoring		
Insect traps	Pheromone trap; light trap; sweet-sour bait trap	MTC
Chemical control		
Recommended active ingredients	Emamectin benzoate (MTLCV); indoxacarb (MTLCV); chlorantraniliprole (MTLC); flubendiamide (MTLC); spinetoram (TLV); methoxyfenozide + spinetoram (TL); chlorfenapyr (TL); lufenuron (TV)	MTLCV
Application		
- Seed treatment	Cyantraniliprole; cyantraniliprole + thiamethoxam	TLV
Insecticide resistance management (IRM)	Alternate use of insecticides with different active ingredients to avoid resistance evolution in pests; switch chemical groups every 30 days	MTLV
Biological control		
Insect natural enemies		
- Egg parasitoids	*Trichogramma* spp.	MTV
- Predators	Earwigs; predatory stink bugs; assassin bugs; ladybugs	TCV
Pathogens		
- Bacteria	*Bacillus thuringiensis* var. *aizawai* or *kurstaki*	MTLV
Conservative biological control	No tillage, retain crop residues, and perform crop rotation to encourage beneficial insects; restrict use of chemical pesticides	MTV
Cultural and interference methods		
Agronomic practices		
- Weeding	Eliminate grassy weeds	MCV
Other methods		
Hand picking	Twice a week when FAW oviposition is heavy, and after that at weekly or fortnightly intervals	MTV

Selected recommended techniques from the six categories of measures, including only those recommended by three or more countries. Country abbreviations: "M" = Myanmar, "T" = Thailand, "L" = Laos, "C" = Cambodia, "V" = Vietnam. In the chemical control category, the names of countries recommending each specific active ingredient are listed.

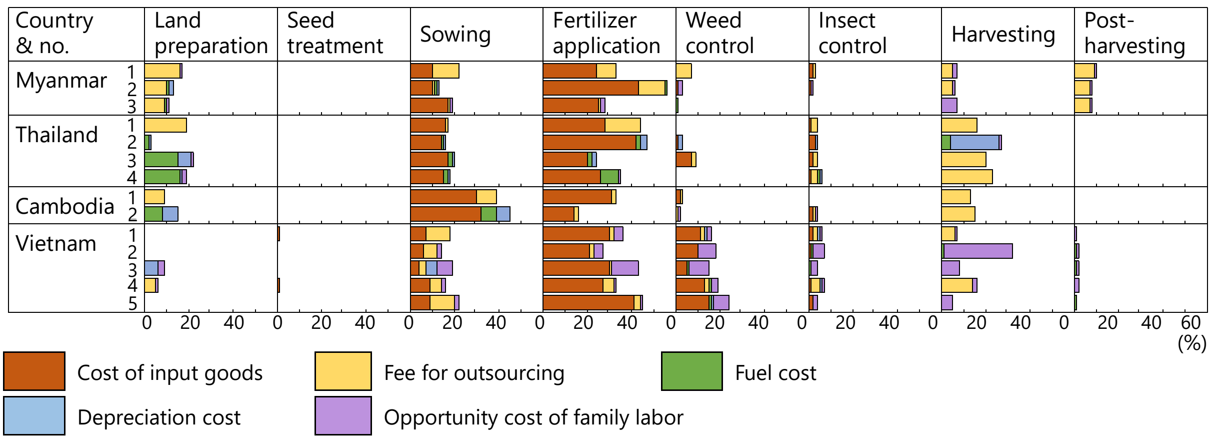

Fig. 1. Proportion of production costs for each maize production stage, wet season, 2022

The horizontal axis is labeled in 10% intervals, with all categories capped at a maximum of 60%. "Insect control" denotes foliar chemical insecticide treatment. "Post-harvesting" includes de-husking, threshing, drying, and transportation of seeds from the field to the market. "Disease prevention and curing" was not included due to zero responses in the survey. Interviews were also conducted in Laos; however, no valid responses were obtained.

Reference: Kusano et al. (2025) *Front Insect Sci* 4: 1455585.

Dense planting enhances grain yield and profitability in low-yielding paddy fields of Sub-Saharan Africa

Rice yields in Sub-Saharan Africa (SSA) average 2.1 t ha^{-1}, which is significantly lower than in other regions. Many smallholder farmers in SSA face economic constraints that limit their access to essential resources for improving yields, such as irrigation facilities, chemical fertilizers, and high-quality seeds. Optimizing planting density is a technique that smallholder farmers can implement on their own without these external inputs.

The effects of planting density have been extensively studied in irrigated rice fields with relatively high yield levels exceeding 5 t ha^{-1}. However, no experimental studies have systematically examined how variations in planting density impact rice yields in low-yielding paddy fields (<5 t ha^{-1}) commonly found in SSA.

This study was conducted in Madagascar, where low-yielding paddy fields are widespread. We examined the effects of two planting density treatments: the standard planting density of 25–26.7 hills m^{-2} (*Standard*) and a doubled density of 50–53.3 hills m^{-2} (*Dense*) using a common variety (X265) in a range of 38 environmental conditions. Additionally, based on household surveys of 356 farmers across 60 villages, we estimated the economic benefits of optimizing planting density by calculating the costs associated with seeds and labor, as well as the revenue gains from increased yields.

The results demonstrated that the dense planting had significantly and consistently higher yields than standard planting by 0.4 t ha^{-1} in the yield range of 1.8 and 4.6 t ha^{-1} while no advantage was detected when the yield was high at 5.5 t ha^{-1} or extremely low at < 1.3 t ha^{-1} (Fig. 1). In the yield range of 1.8 and 4.6 t ha^{-1}, dense planting boosted initial light interception (Fig. 2), and the cumulative light interception from transplanting to maturity was closely correlated with the grain yield (Fig. 3). A household survey identified that the added seed and labor costs for doubling transplanting density from *Standard* to *Dense* were 58,000–62,000 MGA ha^{-1} and 66,000–71,000 MGA ha^{-1}, respectively (Table 1). The additional benefit from the yield gain of 0.4 t ha^{-1} was estimated at 441,000 MGA ha^{-1}, which exceeded 3 times the sum of added seed and labor costs for doubling planting densities. The study provided a practical and impactful strategy for increasing rice yields of smallholder farmers in SSA.

Authors: Tsujimoto, Y., Ozaki, R. [JIRCAS], Andrianary, B.H., Rakotonindrina, H., Ramifehiarivo, N. [University of Antananarivo]

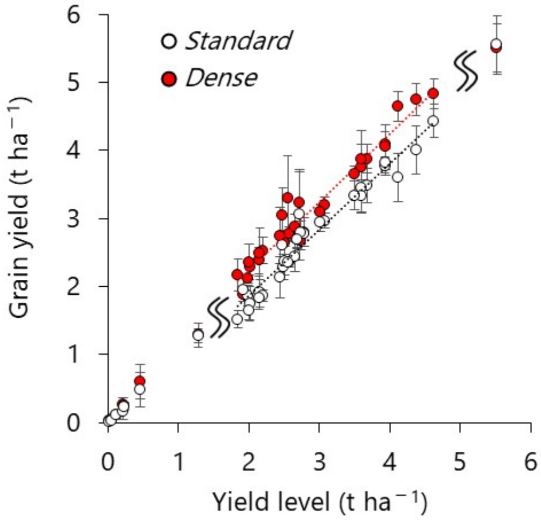

Fig. 1. Effect of transplanting density on grain yield under a range of yield levels

The yield level is the mean yield of two transplanting density treatments. The effect of transplanting density is significant with no interaction of environments in the yield range of 1.8 and 4.6 t ha^{-1} (n=30), but not significant in the other environments (n=8). Errors bars represent the standard error of the replicates.

Copyright 2024 Elsevier

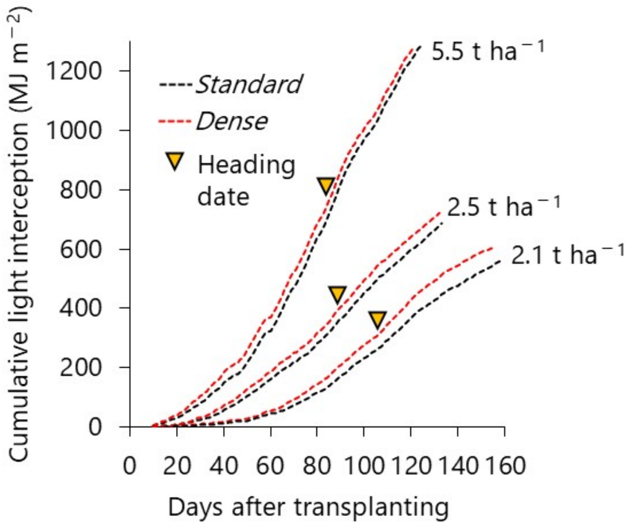

Fig. 2. Cumulative light interception at different yield levels

Cumulative light interception was determined by summing the daily intercepted radiation, which was calculated as the product of daily canopy coverage and solar radiation. The daily canopy coverage was estimated using weekly captured canopy images and the image analysis software ImageJ.

Copyright 2024 Elsevier

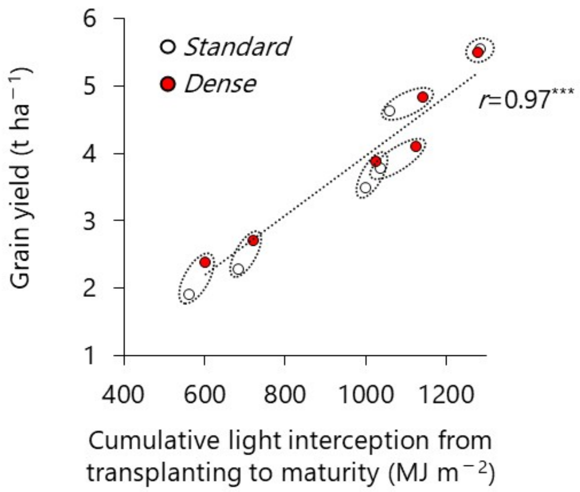

Fig. 3. Correlation between cumulative light interception and grain yield

*** Significant at p<0.001.

Copyright 2024 Elsevier

Table 1. Estimated costs of seeds and transplanting labor for the standard and dense planting treatments

	seed cost (10^{3}MGA ha^{-1})	labor cost for transplanting (10^{3}MGA ha^{-1})
Farmer*	106	120
Standard	58~62	66~71
Dense	116~124	132~142

*Mean of 356 farmers across 3 years. The costs of seeds and transplanting labor were estimated for the standard and dense planting treatments assuming that these costs increase or decrease in direct proportion to planting density. The average planting density of farmers was 45.2 hills m^{-2}.

Reference: Andrianary et al. (2024) *Field Crops Res*. 318: 109601.

The figures and table are modified from Andrianary et al. (2024) © Elsevier B.V.2024

Simple soil diagnostic information increases lowland rice yields and income of smallholder farmers in Madagascar

In sub-Saharan Africa, where farmers face low purchasing power and high spatial variability in soil fertility, targeting fertilizer application to responsive plots is crucial to improve agricultural productivity and income. However, the use of soil diagnostic information remains limited due to the complexity and high cost of generating such data, which involves assessing multiple soil characteristics. Few experimental studies have empirically evaluated the impact of providing soil diagnostic information on farmers' fertilizer use and income. This study focuses on the central highlands of Madagascar, where fertilizer use is low compared to other SSA countries and soil phosphorus deficiency is a major constraint on agricultural productivity. Through a socioeconomic experiment, this study examines the impact of providing smallholder farmers with simple diagnostic information based solely on soil phosphorus content on their fertilizer use, productivity, and income.

In our experiment, soil composites were collected from the focal lowland rice plots of randomly selected 70 households across 10 villages. Oxalate-extractable phosphorus content was analyzed to determine whether the effectiveness of nitrogen application would be high or low. Only 35 households in the treatment group received this binary information before the cultivation period began (Fig. 1). The treatment and control groups were randomly assigned, with no prior differences observed between them in terms of income, plot size, lowland rice yield, chemical fertilizer use, or the proportion of plots where nitrogen application effectiveness was classified as high (Table 1). The results demonstrated that, at the plot level, receiving information that nitrogen application effectiveness was high led to a higher nitrogen application rate and lowland rice yield by 34.1 kg ha^{-1} (76%) and 1.1 t ha^{-1} (24%), respectively, compared to the plots of control group households, where no diagnostic information was provided (Fig. 2). In terms of household-level impacts, the receipt of the binary diagnostic information led to a 0.6 t ha^{-1} (16%) higher rice yield and 434,000 MGA ha^{-1} (24%) higher income for households in the treatment group compared to those in the control group, while the nitrogen application rate did not show a significant difference (Fig. 3).

This study provided insights into policy design to promote efficient fertilizer management, thereby improving farm productivity and income, especially in regions where farmers' purchasing power is limited and soil fertility varies from field to field.

Authors: Ozaki, R., Tsujimoto, Y. [JIRCAS],
Andriamananjara, A., Rakotonindrina, H. [University of Antananarivo], Sakurai, T. [Tokyo Univ.],

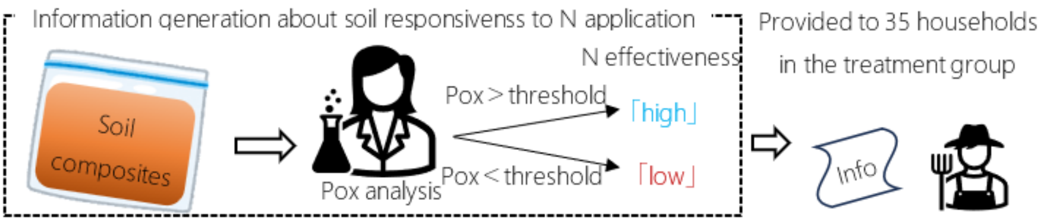

Fig. 1. Process of information generation and provision

Oxalate-extractable phosphorus (Pox) of surface soil was analyzed. Following Asai et al. (2020) *Plant Prod. Sci.* 24 (4): 481–489, N application effectiveness was considered "high" if Pox exceeded 100 ppm, and "low" otherwise. In villages where phosphorus absorption capacity was high due to volcanic ash soil, the threshold was 300 ppm. To prevent differences in conditions and the burden of procuring fertilizer from influencing the results, 5 kg of urea was provided.

Table 1. Situation of target farmers before intervention

	Treatment	Control
1. Household size	5.1	5.3
2. Years of education of household head	5.7	6.3
3. Household income(10^3 MGA)*	638.0	628.7
4. Total size of rice plot including upland rice (ha)	0.61	0.45
5. Size of rice plot subset to soil analysis (ha)	0.17	0.14
6. Yield of the rice plot in the previous year (t ha^{-1})	4.3	4.5
7. N application rate of the rice plot in the previous year (kg ha^{-1})	14.1	13.3
8. Percentage of "high" plots in Nitrogen application effectiveness (%)	28.6	34.3

Differences between the two groups were tested using a *t*-test (1–7) and Fisher's exact test (variable 8). No significant differences were found. *Income was calculated as the value of household assets. N application rate was calculated based on the N content of the chemical fertilizer used. If no fertilizer was used, it was recoded as 0 if none was applied (same calculation for Fig. 2 and Fig. 3).

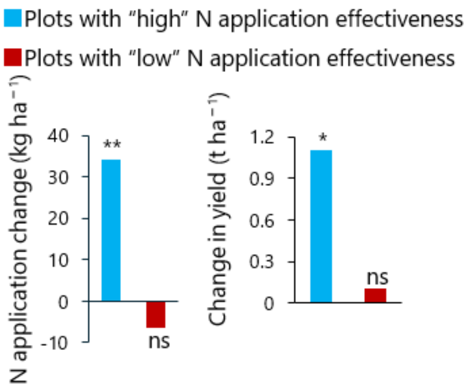

Fig. 2. Impacts of information on N application and yield of the target lowland rice plots

** and * denote p<0.05 and p<0.10, respectively. ns denotes no significance. Changes were estimated as regression coefficients comparing with target plots of the control group.

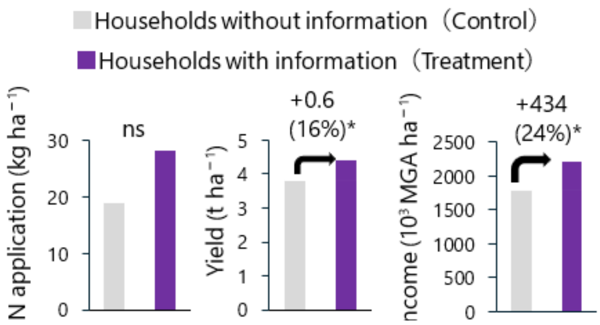

Fig. 3. Impacts of information on N application and yield of the target plots

* and ns denote p<0.10 and no significance, respectively. Income was calculated by subtracting costs of seed, hired labor, fertilizers, and chemicals from the value of products, and converted to per hectare.

Reference: Ozaki et al. (2024) *Agriculture & Food Security* 13: 45.

A quantitative locus, *MP3*, which increases panicle number, enhances grain yield in Hokuriku 193, the highest-yielding rice cultivar for livestock in Japan

In recent years, agriculture and livestock in Japan have become increasingly challenging due to global warming as well as rising fertilizer and feed prices caused by changes in international situations. Under these circumstances, the use of highly productive rice is a possible strategy to stabilize farmers' production and profits. Previously, we identified a quantitative locus, *MP3*, whose Koshihikari allele increased panicle number in the genetic background of *indica* cultivars. A near-isogenic line (NIL) carrying the Koshihikari allele in the genetic background of the high-yielding *indica* cultivar Takanari increased panicle and spikelet number, and enhanced grain yield under an elevated atmospheric CO_2 environment. However, the NIL did not increase grain yield under an ambient CO_2 environment, probably due to its insufficient photosynthetic capacity. On the other hand, another Japanese *indica* cultivar Hokuriku 193, which recorded Japan's highest yield of 13 t ha^{-1}, may have the potential to enhance grain yield with *MP3* under ambient CO_2 environments because it may have surplus photosynthetic ability. The purpose of this study is to develop another NIL carrying *MP3* in the Hokuriku 193 genetic background, and elucidate whether *MP3* contributes to enhancing grain yield in the Hokuriku 193 genetic background under different nitrogen fertilizer applications.

We can see that Hokuriku 193-*MP3*, developed from multiple backcrossing of Koshihikari with Hokuriku 193 (Fig. 1A), shows more matured panicles compared to Hokuriku 193 (Fig. 1B). Hokuriku 193-*MP3* increases panicle number by 21–28% (Fig. 2A) and spikelet number by 22–23% (Fig. 2B) irrespective of nitrogen applications. Then, it enhances grain yield by 6%, from 9.7 t ha^{-1} to 10.3 t ha^{-1} with nitrogen application, and by 8%, from 7.7 t ha^{-1} to 8.4 t ha^{-1} without nitrogen application compared to Hokuriku 193 (Fig. 2C). Non-structural carbohydrate (NSC) content in stems is dramatically decreased in Hokuriku 193-*MP3* compared to Hokuriku 193 during the initial 2 weeks after heading (Fig. 3), suggesting that more NSC is translocated to panicles in Hokuriku 193-*MP3* for promoting the growth of endosperm cells. The percentage of empty spikelets (weighing 6 mg or less) in a panicle is 11% in both Hokuriku 193 and Hokuriku 193-*MP3* (Fig. 4), suggesting that Hokuriku 193-*MP3* has surplus photosynthetic and translocation abilities that can fill the *MP3*-increased spikelets.

Since Hokuriku 193-*MP3* enhances grain yield even with low nitrogen application, the use of Hokuriku 193-*MP3* is expected to contribute to stable rice production for farmers under rising fertilizer prices. Moreover, *MP3* is expected to further improve the yield potential of world *indica* cultivars with high photosynthetic ability equivalent to Hokuriku 193.

Authors: Takai, T., Oo A.Z. [JIRCAS], Nakano, H. [NARO]

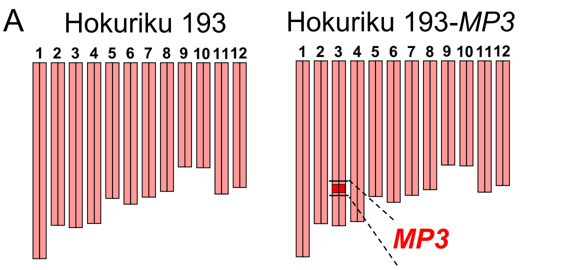

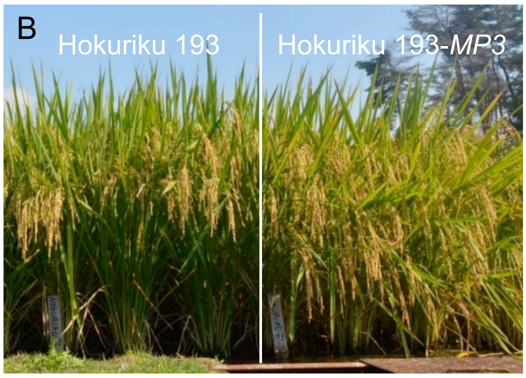

Fig. 1. Development of Hokuriku 193-*MP3*

Genotype (A) and plant appearance (B) of Hokuriku 193 and Hokuriku 193-*MP3*. The number and bar in (A) indicate chromosome number and length, respectively.

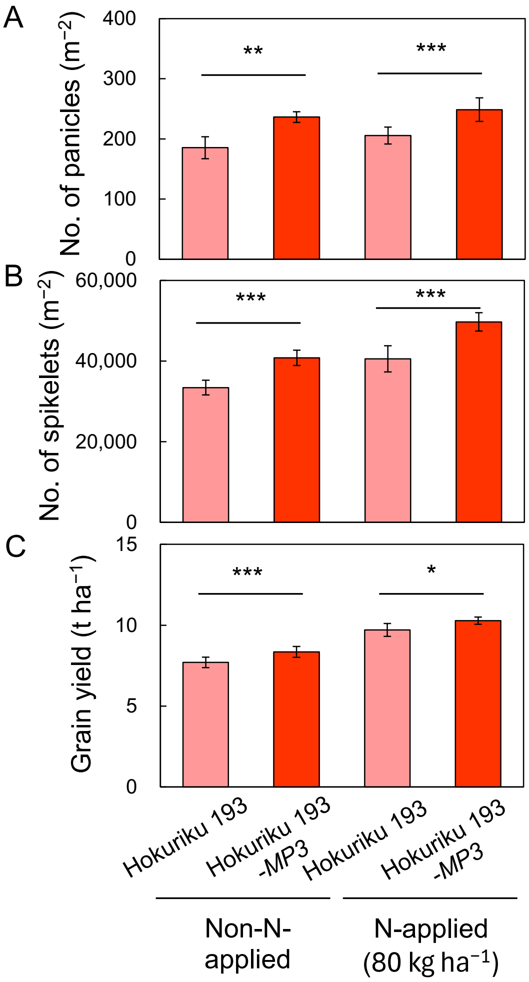

Fig. 2. Comparisons of panicle number (A), spikelet number (B), and grain yield (C) between Hokuriku 193 and Hokuriku 193-*MP3* with and without nitrogen (N) applications

*, **, and *** show significance at 5%, 1%, and 0.1% levels, respectively, by ANOVA.

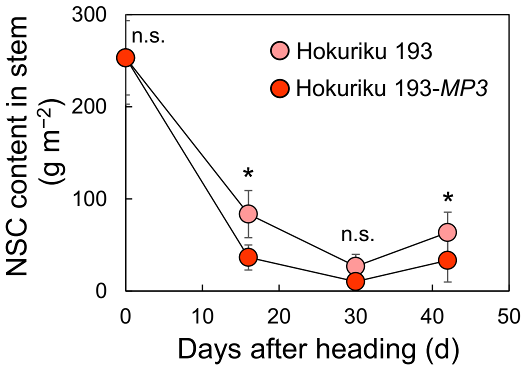

Fig. 3. Comparison of non-structural carbohydrate (NSC) content in stem after heading between Hokuriku 193 and Hokuriku 193-*MP3*

n.s. and * show non-significance and significance at 5% levels by ANOVA.

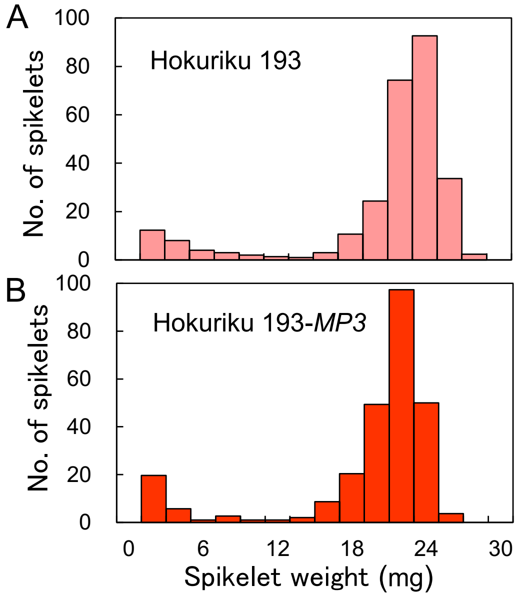

Fig. 4. Distribution of spikelet weight in a matured panicle for Hokuriku 193 and Hokuriku 193-*MP3*

Reference: Takai et al. (2024) *Field Crops Research* 318: 109566.

Enhancing leguminous crop production in semi-arid regions with low-grade phosphate rock as an affordable fertilizer alternative

Phosphorus deficiency in semi-arid tropical soils is a major limitation to food production, causing chronic poverty among smallholder farmers. Chemical fertilizers, which are essential to address this deficiency, are often too costly for farmers in many developing countries, and the recent rise in fertilizer prices has worsened this issue. Low-grade phosphate rocks (Fig. 1), which are rich in impurities and contain lower phosphorus content, are often underutilized. Ground low-grade phosphate rock (referred to as phosphate rock) can serve as a low-cost alternative to chemical phosphorus fertilizers. While phosphate rock's effectiveness has been proven in rice cultivation, its impact on dryland crops is less understood. Leguminous crops, with their ability to fix nitrogen symbiotically and release organic acids that acidify the soil, may be more efficient at utilizing the insoluble phosphorus in phosphate rock. This study aimed to determine the suitability of phosphate rock for five leguminous crops (cowpea, groundnut, bambara nut, soybean, and mung bean) grown in two dominant soil types (Lixisols and Plinthosols) in the Sudan savanna.

Under typical rainfall conditions in the West African dry savanna, applying low-grade phosphate rock from Burkina Faso resulted in similar effects to chemical phosphorus fertilizers for cowpea, groundnut, and soybean (Fig. 2). Among these, cowpea and groundnut showed the highest absolute yields, while soybean, although yielding less overall, exhibited the highest yield increase. The type of soil also affected the results. Lixisols, being more nutrient-rich, produced higher yields than Plinthosols. However, the higher moisture retention in Lixisols led to excessive moisture stress, which reduced the effectiveness of the fertilizer. As a result, the yield increase from phosphate rock application was higher in Plinthosols than in Lixisols.

These findings indicate that low-grade phosphate rock can be an effective and affordable substitute for chemical fertilizers, contributing to improved crop production in low-fertility soils of semi-arid regions. However, the solubility of phosphate rock varies by source, so using more soluble phosphate rocks may yield better results. Additionally, when phosphate rock is applied without nitrogen fertilizers, nitrogen may become the limiting factor, potentially reducing the yield improvement. Therefore, proper nitrogen management is crucial to maximize the benefits of phosphate rock application.

Authors: Iseki, K., Ikazaki, K., Nakamura, S. [JIRCAS], Sidibe, H. [INERA]

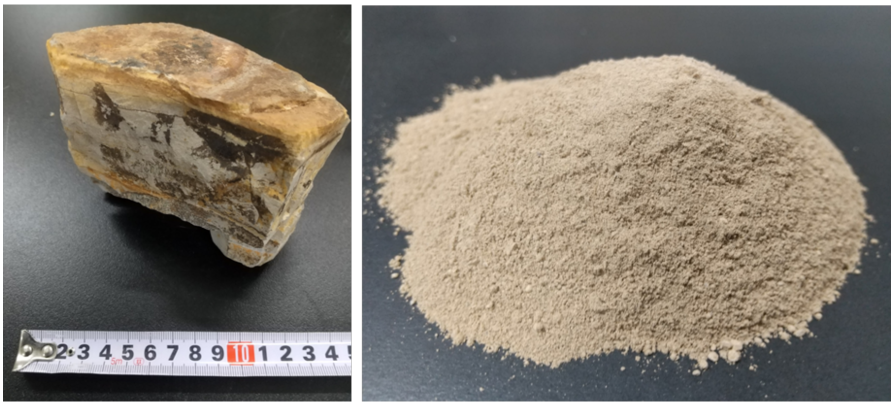

Fig. 1. Low-grade phosphate rock from Burkina Faso (left) and its ground sample (right)

In the field trial, the ground sample on the right was applied at a rate of 400 kg ha^{-1}, following the local recommended application amount.

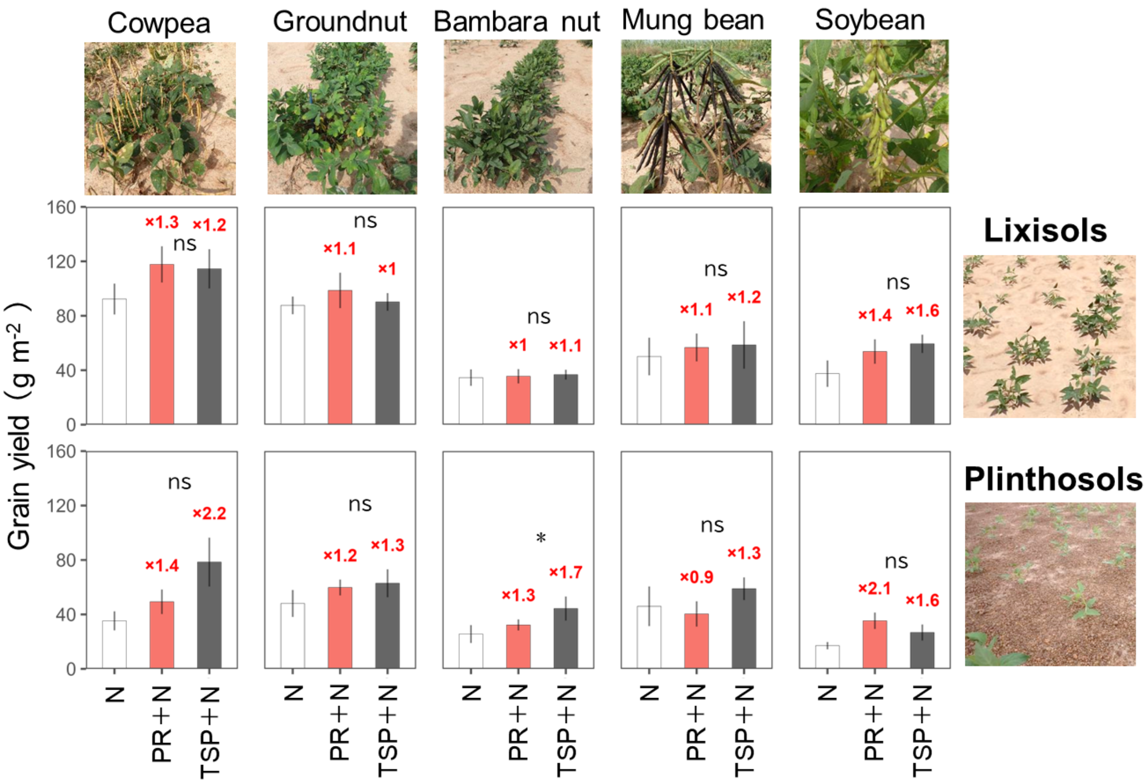

Fig. 2. Differences in the effects of low-grade phosphate rock (PR) and chemical phosphorus fertilizer (TSP) on five leguminous crops

This figure shows the mean ± SE (n=10) from two-year field trials, with five replicates. The control plot received only nitrogen (N) in the form of ammonium at 14 kg ha^{-1}. The treatment plot received chemical phosphorus fertilizer + N, applying a quantity of triple superphosphate (TSP) equivalent to the phosphorus content of the PR (4.6 kg P ha^{-1}). The red text indicates the relative increase in yield compared to the control (N only). "ns" indicates no significant difference in the increase rate between PR+N and TSP+N, while "*" denotes a significant difference at $p < 0.01$ in the increase rate.

Reference: Iseki et al. (2024) *Plant Production Science* 27: 272-282.

A simple evaluation method for seedling emergence ability using soil-gypsum mixed crust

Soil crust, a thin hard layer on the soil surface formed after rainfall, physically inhibits seedling emergence, reducing plant number, which results in cultivation concerns such as reduced yield per unit area and increased cultivation costs due to seed resowing. To cope with this problem, varieties with stable seedling emergence under crust conditions are needed, but testing these materials under crust conditions is difficult because crusts do not form uniformly under natural conditions. In previous research, to reproduce uniform crusts, an artificial rainfall simulator was used with soil from the desired environment. However, this method is not simple due to the labor required for soil collection and the high cost of the artificial rainfall device, making it unsuitable for evaluating a large number of materials at once such as genetic resources. Consequently, previous studies have not been able to evaluate enough number of materials, delaying variety breeding. In this study, we developed a method to evaluate seedling emergence against soil crust conditions using commercial gypsum mixed into soil to reproduce uniform crusts and tested this method on soybean genetic resources.

The method involves mixing commercial gypsum at a ratio of about 20–40% into the soil according to the desired hardness, following sowing of the seeds in paper pots evenly covered with the soil-gypsum mixture (Fig. 1). The paper pots were filled with high water-holding capacity soil (e.g. paddy soil) and the seeds were pre-germinated before sowing to enable highly reproducible evaluation under uniform conditions. Since the soil-gypsum mixture increases in hardness over time, the mixture ratio can be adjusted. We used a 20% mixture ratio since it reached a hardness close to that of the soils prevalent in West Africa (1.57 MPa) after 100 hours of the treatment under 30°C and 50% humidity (Fig. 2). Therefore, since no special equipment is required and the method can be performed at low cost, it is suitable for screening multiple lines with replications (Fig. 3).

This method can be applied to other crops besides soybean by using paper pots of an appropriate size for the seeds. If paper pots are not available, commercial trays can also be used instead. Although the crust hardening speed varies depending on the properties of the soil used and the temperature and humidity conditions after treatment begins, the drying time of the gypsum (set to 100 hours in this study) can be set arbitrarily depending on crop characteristics such as emergence speed and the desired crust hardness.

Authors: Nakagawa, A., Iseki, K., Ikazaki, K. [JIRCAS]

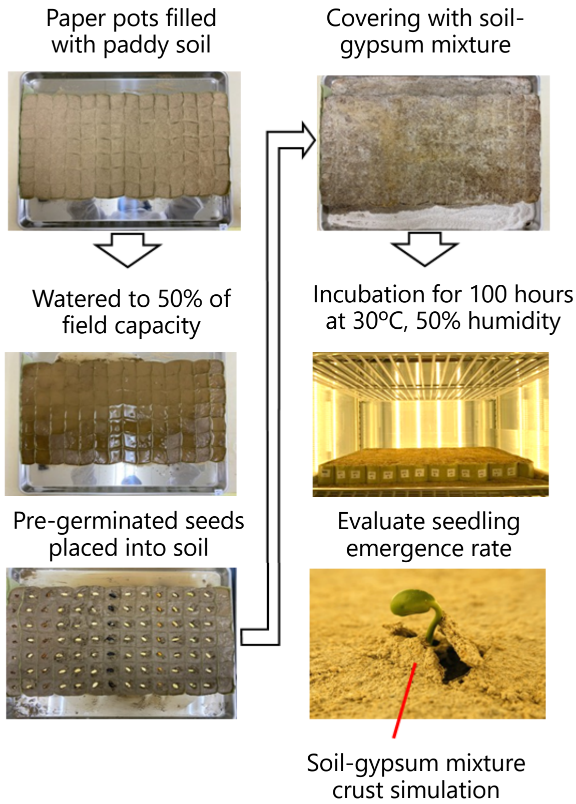

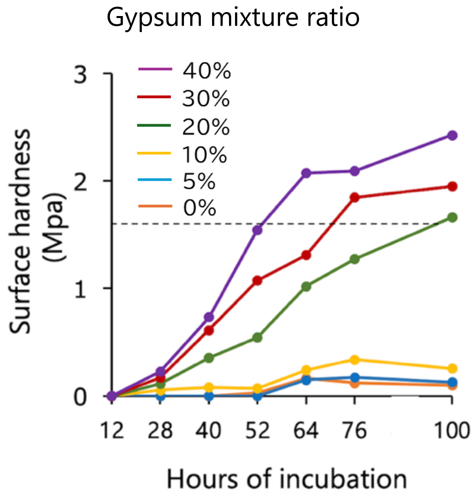

Fig. 2. Temporal changes in surface hardness of soil-gypsum mixture

Changes in surface hardness over time when gypsum was mixed with different ratios (0–40%) measured using a crust hardness meter. The dashed line represents the hardness of the predominant soil of West Africa, the target for this study.

Fig. 1. Evaluation of seedling emergence ability against soil crust

Pre-germinated seeds of soybean were sown in paper pots filled with moisturized paddy soil and covered with soil-gypsum mixture. The paper pots were incubated in a growth chamber at 30°C and 50% humidity and evaluated after 100 hours.

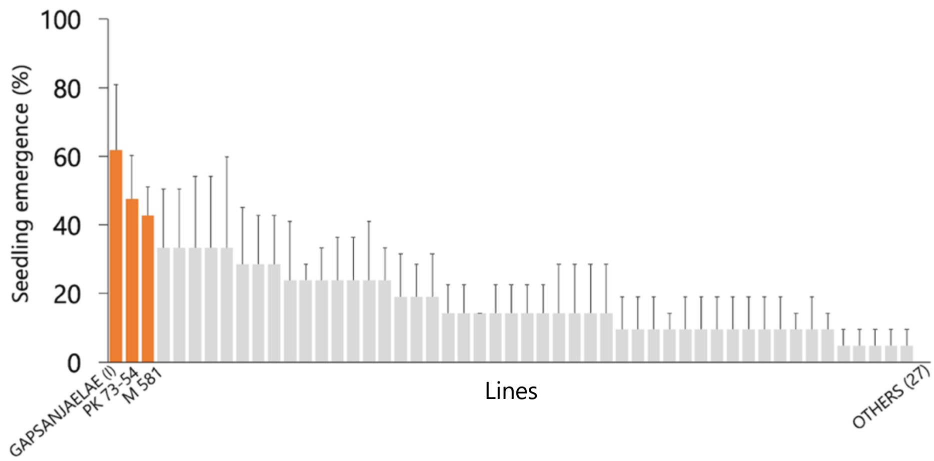

Fig. 3. Evaluation of soybean genetic resources seedling emergence ability using the developed method

Seedling emergence rates of 78 accessions from the World Soybean Core Collection and four tropical varieties. Bars and error bars represent averages and standard errors for three replications, respectively. Orange bars represent the three accessions with the highest emergence rates. Accessions for which seedling emergence rates were zero are shown as 'OTHERS' including 27 accessions.

Reference: Nakagawa et al. (2024) *Plant Production Science* 27(4): 265–271.

Consumers' preferences for nutritional/health, ingredient, and environmental attributes of plant-based meat in China

Rising income and changes in eating habits are driving global meat demand, with OECD/FAO projecting a 14% increase in meat-derived protein demand by 2030. This raises concerns about health and environmental sustainability. Plant-based meat, made from ingredients like soy, wheat, and peas, offers nutritional and environmental benefits as a sustainable alternative. Compared to traditional meat, plant-based meat has a variety of unique attributes, which could be used in promotion. However, since it is not yet widely available on the market, our understanding of consumers' preferences for its attributes is still insufficient. Further research on consumer preferences is needed to promote its widespread adoption. Given that traditional meat consumers are its potential consumers, this study conducted a large-scale consumer survey, which covered 2500 individuals, using the best–worst scaling method (BWS method, Figure 1) in five major cities in China, the world's largest meat and plant-based meat market, as well as the largest meat importer. We selected 13 quantifiable attributes of plant-based meat based on literature review and asked the respondents to identify the most and least favored attributes. Then, we analyzed consumers' preferences for these attributes and examined variations in preference patterns with respect to consumers' socio-demographic characteristics.

Results suggest that consumers prioritized nutritional/health attributes relative to ingredient and environmental attributes, ranking "rich in dietary fiber," "zero hormone," and "zero cholesterol" as the most favored attributes. In contrast, the least favored attributes were "pea protein," "carbon label," and "vegan formula" (Table 1). Using a latent class model, we classified consumers into three groups. Although all groups prioritized nutritional/health attributes, preferences were heterogeneous with respect to socioeconomic characteristics, with younger, higher-income males who spend more on meat favoring healthy nutrients, while others focused on avoiding unhealthy elements of traditional meat (Table 2).

These results could improve our understanding of consumer preferences for plant-based meat and could be used as a scientific basis for policymaking to promote the spread of plant-based meat, thus contributing to the realization of a sustainable and healthy food system. Since nutritional/health attributes were prioritized by consumers, these attributes could be used to attract consumers. Meanwhile, since preferences also varied among consumers, targeted promotional strategies are necessary. Nevertheless, as the survey was conducted in only five major Chinese cities, applying the findings in other contexts requires considering local consumer characteristics.

Authors: Wu, W. [JIRCAS], Yuan, R. [Guizhou Univ.], Jin, S. [Zhejiang Univ.]

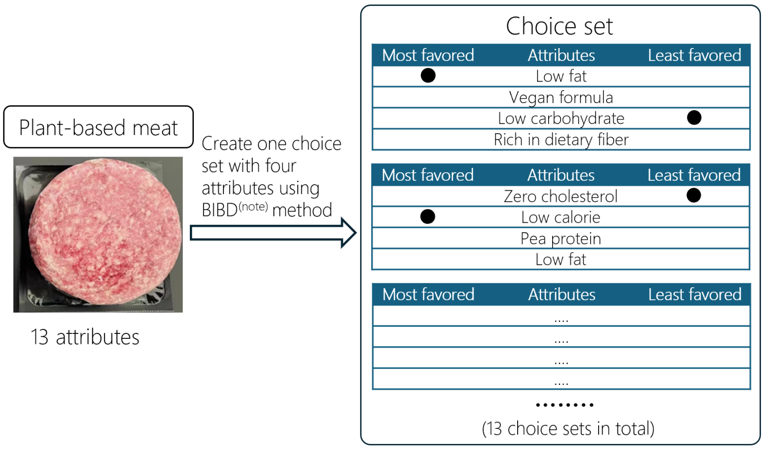

Fig. 1. Examples of BWS choice set presented to respondents

Respondents were asked to select one most and one least favored attribute from each set by marking ●.

(Note) BIBD: Balanced Incomplete Block Design

Attribute	Order of importance	Share of preferences
Rich in dietary fiber	1	17.0%
Zero hormone (note)	2	13.1%
Zero cholesterol	3	11.7%
High protein	4	11.5%
Zero trans fat	5	10.3%
Contains minerals (Fe+)	6	7.3%
Low fat	7	6.7%
Low calorie	8	5.3%
Soy protein	9	4.7%
Low carbohydrate	10	3.7%
Pea protein	11	3.4%
Carbon label	12	2.9%
Vegan formula	13	2.6%

Table 1. Share of preferences estimated by the mixed logit model

Blue: Nutritional/health attributes
Red: Ingredient attributes
Green: Environmental attributes
The share of preferences indicates the percentage of consumers who favor the attribute the most.
(Note) China has banned hormone usage in the livestock sector, but many consumers are still concerned (Wang (2022) *Meat Science* 194: 108982).

Table 2. Consumer segmentation and group characteristics using the latent class model (note)

	Top 3 favored attributes by each group		
Order of importance	Group that prefers healthy nutrients	Group with intermediate preference	Group that dislikes unhealthy elements
1	(+) Rich in dietary fiber	(+) Rich in dietary fiber	(−) Zero hormone
2	(+) High Protein	(−) Zero hormone	(−) Zero trans fat
3	(+) Contains minerals (Fe+)	(+) High Protein	(−) Zero cholesterol
Percentage of consumers	47%	24%	29%
Socioeconomic variables			
Income (7 groups: low to high)	0.19***	0.05	baseline
Age	−0.11**	−0.01	baseline
Gender (female=1, male=0)	−0.24**	−0.24**	baseline
Meat expenditures (4 groups: low to high)	0.43***	−0.01	baseline

(Note) The latent class model could allocate observed individuals to one of the latent classes.
(+) indicates an increase in healthy nutrients by consuming plant-based meat.
(−) indicates a decrease in unhealthy elements by consuming plant-based meat.
** and *** indicate significance at 5% and 1% levels, respectively (Wald-test).

Reference: Wu et al. (2024) *Future Foods* 9: 100384.

Development of a new methodology for controlling maturation in the whiteleg shrimp, *Litopenaeus vannamei*, using live feeds

In order to ensure the sustainability and profitability of whiteleg shrimp production, it is essential to secure a stable supply of high-quality post-larvae. In this study, it was determined that feeding live polychaetes belonging to the *Nereis sp.*, in combination with commercial pellets, is effective in promoting the induction of ovarian maturation in parent shrimp and increasing the number and frequency of spawning occasions.

Eyestalk ablation is employed worldwide in conventional hatcheries for the purpose of inducing maturation and spawning in female spawners. This methodology is effective because it removes the source of vitellogenesis-inhibiting hormone (VIH), allowing maturation to proceed. However, the eyestalks are responsible for the synthesis/secretion of many other important hormones that control essential life processes; eyestalk ablation thus imposes a heavy burden on the animal. Moreover, in recent years, this procedure has been deemed undesirable from the perspective of animal welfare. The overarching aim of this research is to combine feeding methods and hormonal manipulation to offer an alternative technology to the shrimp culture industry.

Four test groups were set up as shown in Figure 1, and nine female spawners were reared under each treatment. The effectiveness of each treatment was evaluated by following the scheme shown in Figure 2. With regard to the total number of times that maturation occurred in each test group, the eyestalk-ablated groups (B, D) showed a frequency 3.0- to 4.3-fold higher than the non-ablated groups (A, C) under the same feeding conditions. This indicates that eyestalk ablation is highly effective, but when the results are considered by comparison among feeding treatments, the use of live feeds yielded results 2.3-fold higher in group C compared to group A (Table 1). In addition, irrespective of whether eyestalk ablation was carried out, in the groups fed live polychaetes, maturation-inducing effects lasted for a longer duration than in individuals fed only commercial pellets (Fig. 3).

In addition, male spawners were employed for the purpose of implementing natural mating or artificial insemination. In terms of the total number of spawnings, group D (eyestalk ablation/live feed administered) showed the highest number of spawnings, but in terms of number of eggs per spawning, group C (eyestalks not removed/live feed administered) showed the highest values (Table 1).

By feeding female spawners with live feed in addition to commercial pellets, it is possible to enhance ovarian maturation and spawning. This is expected to become a component of a new technology that will replace the labor-intensive process of eyestalk ablation, and thus address issues that relate to animal welfare.

Authors: Wilder, M., Kang, B. J., Sultana, Z. [JIRCAS]

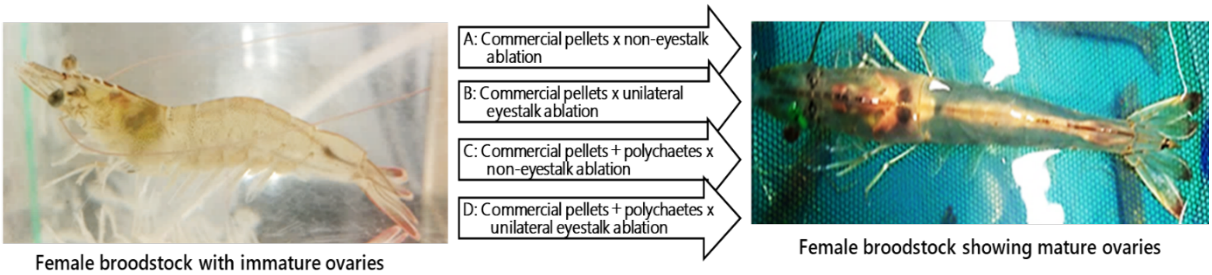

Fig. 1. Experimental design for evaluating the effects of feeding on ovarian maturation in the whiteleg shrimp, *Litopenaeus vannamei*

The effects of four experimental treatments on ovarian maturation were examined in *L. vannamei*. Animals were fed with either commercial pellets only or commercial pellets together with live feed (*Nereis* sp. polychaetes) at a ratio of 3:7. Each feeding protocol was combined with either non-ablation or unilateral eyestalk ablation.

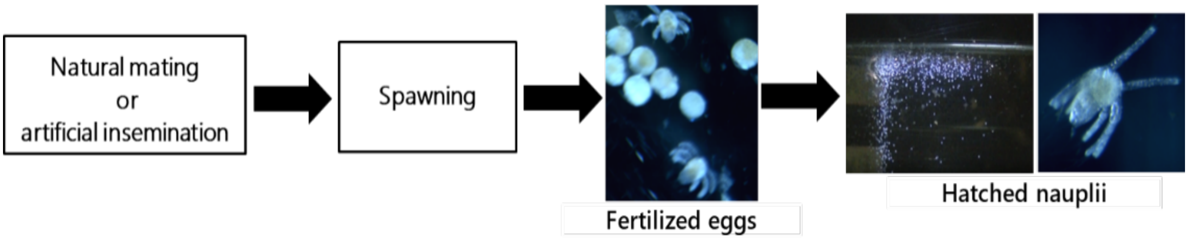

Fig. 2. Scheme for promoting spawning and obtaining fertilized eggs and hatched nauplii via natural mating or artificial insemination in *L. vannamei*

Table 1. Maturation and spawning of whiteleg shrimp (*L. vannamei*) broodstock for each of four experimental treatments

	Commercial pellets		pellets+polychaetes	
	A: pellets x non-eyestalk ablation	B: pellets x unilateral ablation	C: pellets + polychaetes x non-ablation	D: pellets + polychaetes x unilateral ablation
Total number of maturations	3	13	7	21
Total number of spawnings	1 $^{(a)}$	2 $^{(a)}$	4 $^{(b)}$	7 $^{(a)}$
Number of eggs per spawn	$1.4 \times 10^{5\,(-)}$	$(1.3 \pm 0.3) \times 10^{5\,(a)}$	$(4.4 \pm 0.2) \times 10^{5\,(b)}$	$(2.7 \pm 0.2) \times 10^{5\,(a)}$

Results are expressed as the cumulative total of maturation and spawning incidents observed during an eight-week experimental duration (nine female broodstock per treatment), and the average number of eggs per spawning. Differing letters in the table indicate significant difference (One-way ANOVA followed by the chi-square test; $p < 0.05$); "-" indicates that statistical analysis was not performed due to that only one individual spawned under this treatment).

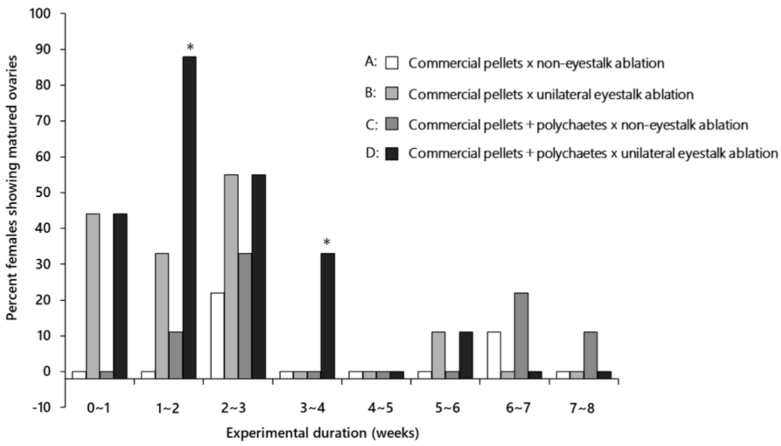

Fig. 3. Percentage of females showing matured ovaries per week for each treatment

Results for each of the four treatments, as detailed in Figure 1 and Table 1, are shown on a weekly basis for the duration of the experimental period. Groups that differ significantly (Friedman test, $p < 0.05$) are indicated with an asterisk.

Reference: Sultana et al. (2023) *Nippon Suisan Gakkaishi* 89: 127–136 (Fig. 1a, Fig. 3a, Table 2, Table 3)

Breeding and variety registration of "Isan," the first *Urochloa* grass variety for the Asian monsoon

Urochloa (formerly known as *Brachiaria*) is a tropical grass widely grown in tropical and subtropical regions of the world. It has excellent forage characteristics such as high yield, strong drought resistance, aptitude for grazing, and high crude protein content. However, the breeding of *Urochloa* has been limited, only about 20 varieties have been registered in the world, most of which were bred in South America and Australia, and no varieties have been bred for the Asian monsoon region. On the other hand, beef and milk production is increasing in this region, and livestock farmers are under pressure to develop efficient feed production technology. Therefore, we will breed and develop tropical grass varieties that are suitable for the Asian monsoon climate and can be cultivated at a low cost with high yield and high quality.

"Isan" is the first variety of *Urochloa* pasture grass in Japan and Thailand (Figs. 1 and 2). Figure 3 shows the background of the breeding process and the roles of each organization. It has an average dry matter yield of 18.8 t ha^{-1} per year, about 12% higher than the average of 16.8 t ha^{-1} of existing varieties (Table 1). The dry matter ratio is about 2% lower than that of the existing varieties. It has excellent crude protein content, about 3% higher than the existing variety "Kennedy" at 17.2% in the first crop of the first year, and the TDN (Total Digestible Nutrients) content is similar to the existing variety. It can be easily established as a highly uniform pasture from seed due to apomixis.

"Isan" is distinguished by its high yield, high quality, and easy management, and has high potential to meet the needs of pasture grasses in the Asian monsoon region. In the frost-free zone of the Nansei Islands in Japan, it can be used as permanent grazing pasture or meadow. Because of its high crude protein content and suitability for rough grazing, it is expected to help farmers stabilize their business by reducing the need to purchase concentrate feeds, which are becoming increasingly expensive. The high summer temperatures in recent years have caused summer depression of temperate grasses. It is resistant to high temperatures and drought, and can reproduce by seed, so it is expected to be used in pastures from Kyushu to the Kanto region for a single year. Pre-drying is required to adjust moisture content to 60–70% for silage preparation due to its low dry matter content.

Authors: Shimoda, K. [NARO], Ando, S. [JIRCAS], Ebina, M. [NARO], Kouki, K. [Okinawa Pref.], Akashi, R. [Miyazaki Univ.], Suenaga, K. [JIRCAS], Ando, S. [NARO], Kanamori, N., Matsumoto, N. [JIRCAS], Nakamanee, G., Rimkeeree, K., Srisompom, W., Patipan, C., Mangpung, Y. [DLD]

Table 1. Key characteristics of "Isan" and control varieties

	Isan	Kennedy	Mulato II
Dry matter yield (t ha^{-1} y^{-1})			
1st year	22.7 a	20.7 b	19.6 b
2nd year	14.8 a	13.3 b	13.6 ab
2-year average	18.8 a	17.0 b	16.6 b
Dry matter ratio (%)			
1st year	17.5 b	19.9 a	18.3 ab
2nd year	20.4 b	22.1 ab	23.6 a
Feed ingredients (%)			
Crude protein	17.2 a	14.3 b	16.1 a
Crude fat	2.5 a	2.0 a	2.3 a
Crude ash	14.3 a	13.8 ab	13.0 b
ADF	34.3 a	31.0 a	32.3 a
NDF	59.5 a	60.3 a	55.6 a
ADL	3.3 a	2.9 b	3.2 a
TDN	61.3 a	61.9 a	61.9 a
Parthenogenesis (%)			
Embryo sac analysis	86.4	0.0	90.3

Note: Unpublished data (from Shimoda)

Fig. 2. Local adaptation test field at Nakhon Ratchasima Livestock Nutrition Research and Development Center (Pak Chong)
The area indicated by white arrows is the "Isan" plot (photo taken in September 2014).

Fig. 1. Grass form of "Isan"

Crossbreeding between "Miyaokikuni 1," a sexually reproduced tetraploid Ruzigrass intermediate parent created by chromosome doubling by the Faculty of Agriculture, University of Miyazaki, as seed parent and "Mulato," an apomixis hybrid transferred from the International Center for Tropical Agricultural Research (CIAT), as pollen parent at JIRCAS (2008–2009).

↓

Selection and determination of apomixis of the obtained crosses at the Nasu Research Station, Institute of Livestock and Grassland Science, National Agriculture and Food Research Organization (2010).

↓

Evaluation of agricultural characteristics at the Nakhon Ratchasima Livestock Nutrition Research and Development Center, Department of Livestock Development (DLD), Ministry of Agriculture and Cooperatives, Thailand (2011–2012).

↓

Local adaptation test of the three selected strains was conducted at five DLD-affiliated research centers in Thailand, including the Center, and the Okinawa Prefectural Livestock Research Center in Japan, to evaluate drought resistance in areas with severe dry seasons. Variety characteristics test was conducted at two locations, at the Center and at the Okinawa Livestock Research Center, and the final selection was made (2013–2014).

↓

JIRCAS applied for variety registration (March 2017), established criteria for variety registration examination (March 2020), and registered the variety in Japan (August 2021).

↓

DLD established criteria for variety registration examination (2020), applied for variety registration (May 2021), and registered the variety in Thailand (July 2024).

Fig. 3. Breeding history of "Isan" and the roles of each organization

Reference: Nakamanee et al. "Isan" Variety Registration No. 0924/2024 (2024/7/26 in Thailand).
Shimoda et al. "Isan" Variety Registration No.28580 (2021/8/5 in Japan).

Hybrid sterility between Asian and African rice can be mitigated by tetraploidization

Almost all rice varieties cultivated worldwide belong to the Asian rice (*Oryza sativa*), and modern rice varieties with high yielding capacity and good eating quality are developed through intraspecific crosses within *O. sativa*. In contrast, the African rice (*O. glaberrima*), cultivated only in limited regions of West Africa, exhibits distinct traits such as resistance to certain pests and diseases and adaptability to low-fertility soils. Hybridizing these two species may enable the development of varieties that can be cultivated in environments where *O. sativa* cultivation has been difficult. However, interspecific F_1 hybrids between *O. sativa* and *O. glaberrima* exhibit severe sterility of pollen grains (hybrid sterility), preventing seed production; thus, it is essential to develop fertile interspecific hybrids to overcome this sterility.

In this work, we investigated the relationship between hybrid sterility and ploidy level of the hybrid and found that tetraploid F_1 hybrids can restore pollen fertility and set seeds by self-pollination.

We examined the pollen fertility of F_1 hybrids between an *O. glaberrima* variety (Og) and three *O. sativa* varieties (Os1, Os2, and Os3 belonging to the *temperate japonica*, *indica*, and *aus* subspecies, respectively), and found that while diploid F_1 hybrids showed 0% pollen fertility (complete sterility), tetraploid F_1 hybrids exhibited pollen fertility ranging from 5.7% to 28.1%, enabling self-pollination (Fig. 1).

Genetic analysis of the fertile microspores in the tetraploid hybrids provided insight into the fertility restoration mechanism (Fig. 2). For example, in the *S2* locus, which is one of the loci inducing pollen grain sterility in the hybrid, all microspores carrying the *S2* allele from *O. glaberrima* would be sterile in diploid hybrids. However, they could maintain fertility in the tetraploid situation by carrying the *S2* allele from *O. sativa* simultaneously.

These results suggest that employing tetraploid hybrids can facilitate genetic exchange between the two species, allowing for the development of diverse hybrids with valuable traits, which was difficult in the diploid situation. Furthermore, diploid hybrids between the two species could be developed successfully by rescuing the fertile microspores in the tetraploid hybrid through anther culture methods. Further investigation on pollen fertility and agronomic traits of these diploid hybrids will be required to estimate their usability as hybrids with intermediate genomic compositions between the two species.

Authors: Kuniyoshi, D. [JIRCAS], Ishihara M., Yamamori K., Koide Y., Kishima Y. [Hokkaido Univ]

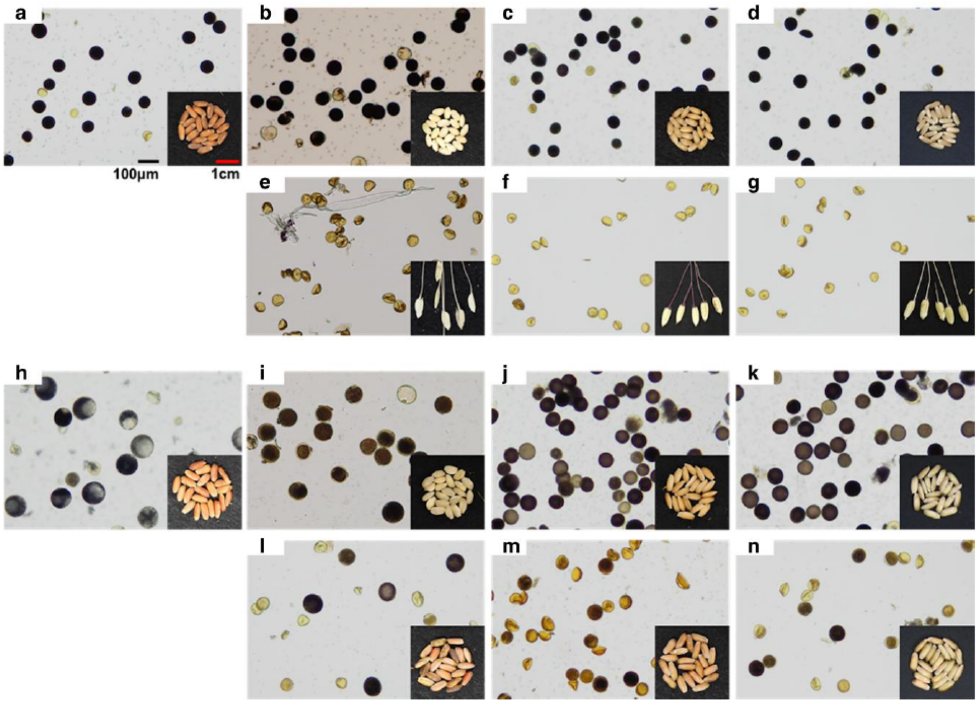

Fig. 1. Observation of fertility of pollen and self-pollinated seeds

Pollen samples were stained with I_2-KI staining then observed. Fertile pollen: black color. Sterile pollen: yellow to brown color.

a–g: Pollen and seeds in the diploid materials.

a: *O. glaberrima* variety (Og); b–d: *O. sativa* varieties (Os1, Os2, Os3). Os1, Os2, and Os3 belong to *temperate japonica*, *indica*, and *aus* subspecies, respectively.

e–g: Og/Os1, Og/Os2, Og/Os3 F_1 hybrids. Diploid hybrids were pollen-sterile, resulting in no seed set.

h–n: Pollen and seeds in the tetraploid materials.

h: Og; i–k: Os1, Os2, and Os3.

l–n: Og/Os1, Og/Os2, and Og/Os3 F_1 hybrids in the tetraploid situation. Pollen fertility was restored in the tetraploid situation; thus, self-pollinated seeds were obtained for all three combinations.

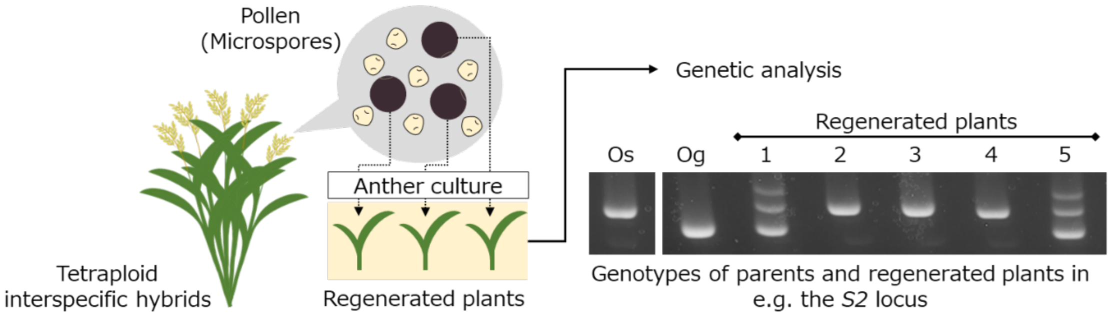

Fig. 2. Genetic analysis of hybrid sterility loci

Diploid plants were produced from fertile microspores of the tetraploid hybrids and analyzed. The hybrid sterility loci (e.g. the *S2* locus) which induce sterility of pollen were targeted for this analysis. The image of gel electrophoresis represents the result of analysis of the *S2* locus: among the plants induced from the fertile micropores, three plants (2, 3, and 4) carried the *S2-Os* allele while two (1 and 5) carried both *S2-Os* and *S2-Og*. Basically, microspores carrying the *S2-Og* allele would be sterile, but this result confirmed that they could maintain fertility in the tetraploid hybrid by carrying it with the *S2-Os* allele.

Figure 1 was reprinted with permission from Oxford University Press, based on the following paper:
Kuniyoshi et al. (2024) Tetraploid interspecific hybrids between Asian and African rice species restore fertility depending on killer–protector loci for hybrid sterility. *GENETICS* 228: iyae104.

High water-use efficiency and associated accumulation of leaf metabolites in *Erianthus arundinaceus*

Erianthus arundinaceus (hereafter, *Erianthus*), a genetic resource of a closely related genus of sugarcane (*Saccharum* spp.), is believed to contribute to the improvement of drought tolerance in sugarcane through intergeneric crosses. However, there has been insufficient verification of the physiological determinants of drought tolerance in this species through comparison with sugarcane, and no progress has been made in searching for promising traits as selection indicators for drought tolerance. Research is needed on drought tolerance-related traits of this species, focusing not only on the root system but also on above-ground characteristics. Leaf water-use efficiency (WUE), which is the photosynthetic rate divided by the stomatal conductance, is considered to be one of the useful indicators. Here, in addition to WUE, we focus on related stomatal morphology and metabolites.

In a glasshouse at the TARF-JIRCAS, a pot experiment was performed under dry and wet conditions to investigate the response of WUE, primary metabolites in various plant parts by metabolomics, and stomatal morphology in sugarcane cultivar NiF8 and *Erianthus* accession JW630, and to search for useful traits in above-ground parts related to drought tolerance (Fig. 1).

Metabolomics of various plant organs and multivariate analysis (principal component analysis, hierarchical cluster analysis) showed that there is a linkage between parts of the plant with regard to metabolite composition, with interspecific differences and soil moisture effects clearly evident, particularly in the leaves. Regardless of soil moisture conditions, *Erianthus* exhibited higher WUE (Fig. 2a) and had fewer stomata on the lower side of its leaves (Fig. 2b). It also accumulated abundant betaine and γ-aminobutyric acid (GABA) in its leaves, which are involved in stomatal closure and stress responses (Fig. 3).

In addition to the known rooting ability, such as deep rooting, the above-ground leaf characteristics (stomatal density, metabolites) may be useful evaluation indicators with regard to the drought tolerance of *Erianthus*. On the other hand, the causal relationship between the high WUE of *Erianthus* (Fig. 2a) and the leaf traits should be investigated further. As a group of genetically distinct genotypes of *Erianthus* is known to exist, it is possible that there are genotypes that show different physiological responses to the present study, and studies focusing on the diversity of traits in the genetic resource population are underway. In the future, the possibility of simple selection for drought tolerance using these traits (stomatal density, leaf metabolites) as biomarkers will be tested using hybrid populations, etc., to improve the efficiency of drought tolerance breeding through the development of drought tolerance-related genetic markers.

Authors: Takaragawa, H. [JIRCAS], Wakayama, M. [Ehime Univ.]

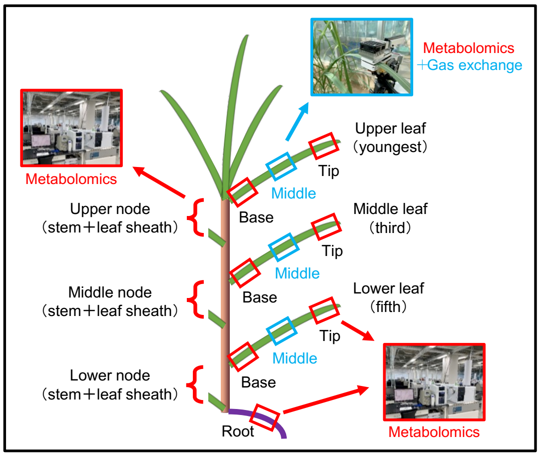

Fig. 1. Targeted plant parts for analysis in the present study

Gas exchange characteristics and stomatal morphology were targeted in the middle parts of the upper, middle, and lower leaves. For metabolomics, a total of 16 samples per plant were tested: nine leaves + three stems + three leaf sheaths + one root. All were sampled from the main stem.

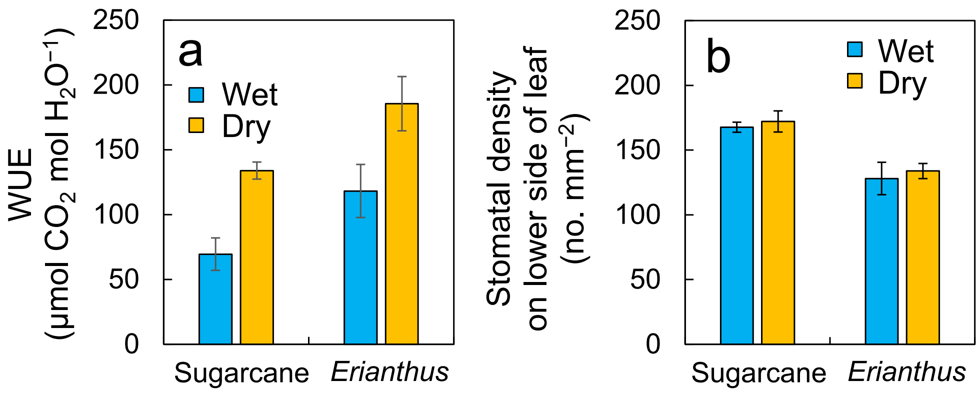

Fig. 2. Interspecific differences in water use efficiency (WUE) calculated from leaf gas exchange parameters (a) and stomatal density on the lower side of leaf (b)

Blue and orange bars represent soil wet and dry treatments, respectively. Error bars represent standard deviations (n=4). These are the measured values for the middle-aged leaves. WUE was measured at a light intensity of 500 μmol m^{-2} s^{-1}. Interspecific differences are significant for each variable in each treatment (*t*-test, $p<0.01$).

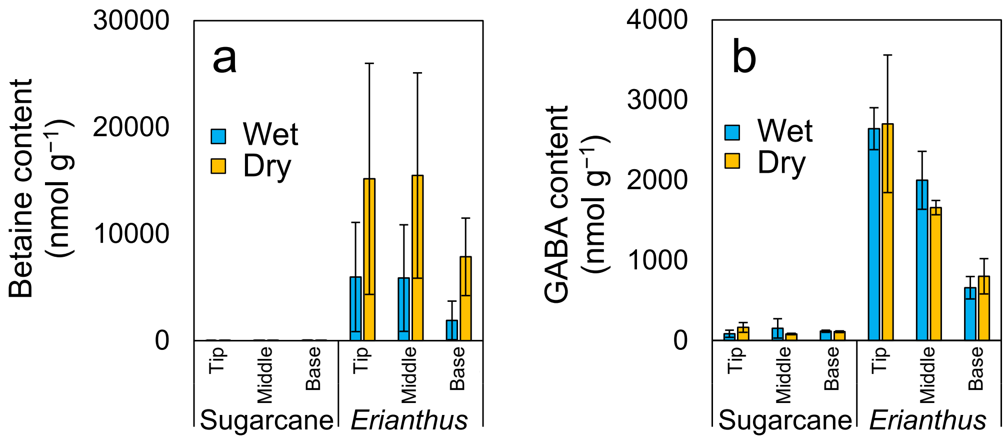

Fig. 3. Interspecific differences in betaine content (a) and GABA content (b) at different leaf parts (tip, middle, and base).

Blue and orange bars represent soil wet and dry treatments, respectively. Values are the means of three leaves; error bars represent standard deviations (n=3). Significant interspecific differences are found for each variable in each treatment (*t*-test, $p<0.05$), except for betaine in the wet plot.

Reference: Takaragawa & Wakayama (2024) *Planta* 260: 90.

DNA markers for assisted selection of cassava resistant to cassava mosaic disease (CMD)

Cassava (*Manihot esculenta*) is an important crop cultivated in tropical and subtropical regions. The stable production of cassava is crucial for food security, as its starch is used in both food and industrial applications. However, cassava mosaic disease (CMD), a viral disease, has significantly hampered cassava productivity, particularly in Africa, India, and recently in Southeast Asia. Developing CMD-resistant cassava varieties is essential, but traditional breeding methods are time-consuming and costly. Therefore, there is a need for DNA markers that can identify the mutations providing CMD resistance to accelerate and reduce the cost of breeding resistant varieties.

As a result, the authors have confirmed mutations in the DNA polymerase δ subunit 1 (*MePOLD1*) gene, associated with CMD resistance, in cassava varieties and lines maintained by the Agricultural Genetics Institute (AGI) in Vietnam. These mutations, G680V and L685F, were found in lines introduced from the International Center for Tropical Agriculture (CIAT) in Colombia and the International Institute of Tropical Agriculture (IITA) in Nigeria, respectively. The developed DNA markers can distinguish these *POLD1* genotypes using two methods: the dCAPS method, which is cost-effective, and the KASP method, which is suitable for high-throughput screening. Field trials in CMD-infected areas showed that cassava lines with the G680V mutation exhibited significantly less severe symptoms compared to non-mutated lines, demonstrating the effectiveness of the DNA markers.

In terms of applications, the developed DNA markers enable the efficient selection of CMD-resistant cassava, thereby facilitating the breeding of varieties suited to conditions in Southeast Asia. These tools can be applied not only to combat CMD in Southeast Asia but also to develop resistant varieties against CMD races prevalent in Africa.

Authors: Tokunaga, H. [JIRCAS], Nhan, P.T., Hoa, T.M., Trang, N.T.H., Tung, N.B. [HLARC],
Huong, P.T, Anh N.H., Huong, L.T.M., Ham, L.H. [AGI],
Thuy, C.T., Zhang, X. [CIAT], Seki, M. [RIKEN]

A Southeast Asian variety (CMD-susceptible) C-33 (CMD-resistant)

Fig. 1. Cassava mosaic disease-resistant varieties

Cultivation of cassava in CMD-infected fields in Vietnam for three months. While the typical Asian variety exhibits CMD symptoms, the C-33 line grows without any disease symptoms. Photo provided by Thuy, C. T. (CIAT).

Table 1. Mutations in the *PLOD1* genes in CMD-resistant varieties and lines

Variety/Line	CMD susceptibility	Mutations in *POLD1* and corresponding amino acid replacements: 680th amino acid – Codon	680th amino acid – Amino acid	685th amino acid – Codon	685th amino acid – Amino acid
Asian varieties	Susceptibility	G G T	G	T T G	L
CIAT lines from Colombia	Resistance	G T T	V	T T G	L
IITA varieties from Nigeria	Resistance	G G T	G	T T C	F

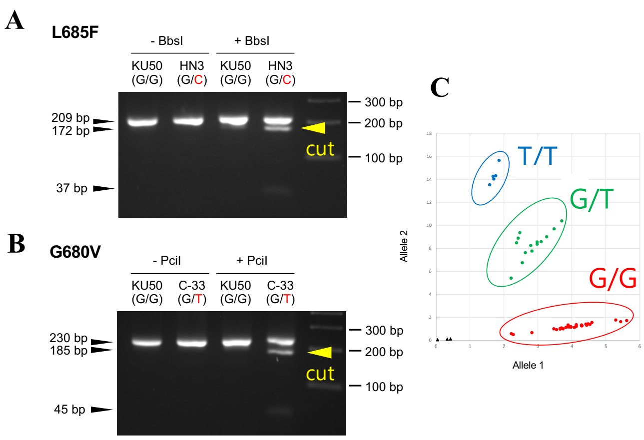

Fig. 2. Identification of *POLD1* mutations using DNA markers

(A, B) The dCAPS method creates restriction enzyme sites into PCR products, identifying *POLD1* gene mutations in WT (KU50), L685F (HN3), and G680V (C-33). PCR products treated with BbsI (A) or PciI (B) show WT if not cut, mutant type if cut. (C) The KASP assay rapidly identifies WT and G680V mutant *POLD1* genes, classifying individuals into WT G/G, heterozygous G/T, and homozygous T/T.

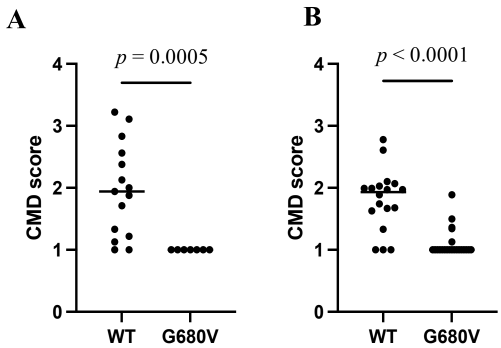

Fig. 3. Association between *POLD1* genotype and CMD resistance

(A, B) Observed CMD symptoms in progeny of G680V-resistant lines crossed with Southeast Asian (A) or South American (B) varieties after 3 months in CMD-infected fields. CMD symptom score 1 indicates no symptoms; higher scores indicate more severe symptoms. Significant differences in CMD scores were found between normal and G680V *POLD1* genes using the dCAPS method.

Reference: Tokunaga et al. (2025) *Breeding Science* (in press).

Japan International Research Center for Agricultural Sciences

Headquarters (Tsukuba)
1-1 Ohwashi, Tsukuba, Ibaraki
305-8686, JAPAN
TEL : +81-29-838-6313
FAX : +81-29-838-6316

Tropical Agriculture Research Front (TARF)
1091-1 Maezato-Kawarabaru, Ishigaki
Okinawa, 907-0002, JAPAN
TEL : +81-980-82-2306
FAX : +81-980-82-0614

https://www.jircas.go.jp/